PHYSICAL LAYER ISSUES OF COMMUNICATION VIA DIFFUSION FOR BIO-NANOMACHINES

by

Mehmet Şükrü Kuran

B.S., Computer Engineering, Yıldız Teknik University, 2004

M.S., System and Control Engineering, Boğaziçi University, 2007

Submitted to the Institute for Graduate Studies in
Science and Engineering in partial fulfillment of
the requirements for the degree of
Doctor of Philosophy

Graduate Program in Computer Engineering

Boğaziçi University

2012

ACKNOWLEDGEMENTS

First of all I would like to thank to my mother, Lale Kuran who has shown me a clear path on how to live as an exemplary human being both with her actions and words amidst all the complexities of the current times we live in. Although, I try to adhere to her teachings and guidelines, I am still but a mere pupil who is very stubborn and impatient.

Second, I would like to thank to my thesis supervisor Assoc. Prof. Tuna Tugcu for the support and help he has given me to work on an extremely new and risky field such as Molecular Communication. I also want to express my gratitude to Dr. Bilge Ozerman and my friend and colleague H. Birkan Yilmaz for the countless hours of discussions, comments, and ideas in a highly multi-disciplinary field such as Molecular Communication. Without their help and feedback this thesis will not come into fruition.

Also, I would like to thank to current and former members of Network Laboratory (NETLAB), Satellite Laboratory (SATLAB), and NaNoNetworking Center in Catalunya (N3CAT) for their support and help during the thesis.

Finally, I would like to thank to my close friends, Burak Pilavcı, Erdost Ansal, Neşe Alyüz, Can Erdamar, Selin Gürsoy, Burak Doğruöz, İlker Kopan, Baki Can Kadıoğlu, Yiğit Sevinç, and Cömert Tülümen for their support before and during this thesis. I would like to thank Emrecan Çakır for the biology illustration he has provided for me for the exocytosis figure in this thesis.

This research is supported by the Scientific and Technical Research Council of Turkey (TÜBİTAK) under grant number 112E011, State Planning Organization of Turkey under grant number 2007K120610, "TAM" project, and Bogazici University Research Fund (BAP) under grant number 6024.

ABSTRACT

PHYSICAL LAYER ISSUES OF COMMUNICATION VIA DIFFUSION FOR BIO-NANOMACHINES

Nanonetworking is a new communication paradigm that focuses on communication between nanomachines. Among the various methods that are being proposed in the context of this paradigm, we focus on the Communication via Diffusion system in this thesis. Modeled after molecular release based communication between neighboring cells in living organisms, this system is currently one of the most prominent systems envisioned to be used between bio-nanomachines. While there are some studies on this system in the literature, most of them focus on a single aspect of the system. In contrast, in this thesis we start with a basic channel model and consider several physical layer issues built upon this channel model. The unique probabilistic medium used in this system requires revisions in physical layer issues (e.g., channel modeling, interference analysis) specific to this medium. We firstly develop a joint channel and energy model to evaluate the capacity of this system. Then, we propose two different modulation techniques and elaborate on the effects of the interference sources (namely the Intersymbol and Co-channel Interferences) over the channel capacity. We also show the importance of the release point selection in this system. Our results show that this communication system is expected to be a good solution between bio-nanomachines that are 1 to 10 μm apart, beyond which the performance of the system degrades quickly. Lastly, we give an overview and future directions of a more controlled diffusion based system, called Calcium Signaling, that is expected to be used in applications where the distance between the transmitting bio-nanomachine pair is longer than 10 μm and there are many devices in the environment.

ÖZET

BİYONANOMAKİNELER İÇİN DİFÜZYON İLE HABERLEŞMEDE FİZİKSEL KATMAN MESELELERI

Nanoağlar nanomakineler arasındaki haberleşme üzerine yoğunlaşan yeni bir haberleşme kavramıdır. Bu tezde, bu konu dahilinde önerilen bir çok haberleşme sisteminin içinden Difüzyon İle Haberleşme sistemi üzerine yoğunlaştık. Bu sistem, biyolojik hücreler arasında molekül salınımı tabanlı haberleşmeden esinlenilerek geliştirilmiştir. Difüzyon ile haberleşme, biyonanomakineler arası kullanım için düşünülen sistemler arasında en önde gelenler arasındadır. Literatürde bu sistem üzerine yapılmış bazı çalışmalar bulunmakta, ancak bunların bir çoğu sistemin sadece tek bir özelliğine yoğunlaşmaktadır. Bu çalışmaların aksine, bu tezde, önce temel bir kanal modeli ile başlayıp sonra bu model üzerinden belli başlı fiziksel katman meselelerini ele alacağız. Bu sisteme ait özel olasılıksal haberleşme ortamı, bir çok fiziksel katman konusunun tekrar gözden geçirilmesi ve incelenmesini gerekli kılmaktadır (ör: kanal modeli, girişim analizi). Öncelikli olarak ortak bir kanal ve enerji modeli geliştirip sistemin kapasitesini hesaplayacağız. Ardından bu sistem için iki modülasyon tekniği önerip bir kısım girişim kaynaklarının (Semboller arası ve Kanallar arası) kanal kapasitesi üzerindeki etkilerini inceleyeceğiz. Ayrıca bu sistemde moleküller için salınım noktası seçiminin önemini göstereceğiz. Sonuçlarımıza göre bu haberleşme sisteminin birbirinden 1 ila 10 μm uzaklıkta olan biyonanomakineler için iyi bir çözüm olması beklenmektedir. 10 μm'nin ötesinde sistemin başarımını hızlıca düşmektedir. Son olarak daha kontrollü difüzyon temelli bir sistem olan Kalsiyum Sinyalleşmesine genel bir bakış atıp bu sistem üzerine gelecekte neler yapılabileceğinden bahsedeceğiz. Kalsiyum sinyalleşmenin aralarında 10 μm'den daha uzun mesafeler olan çok sayıda biyo-nanomakineden oluşan uygulamalar için kullanılması öngörülmektedir.

TABLE OF CONTENTS

LIST OF FIGURES

LIST OF TABLES

LIST OF SYMBOLS

b	Bits per symbol rate
b_{drag}	Drag constant
C	Channel capacity
c_v	Vesicle capacity of messenger molecules
d	Distance between the receiver and transmitter
D	Diffusion coefficient
$E(P)$	Average P distance
E_C	Energy cost of carrying a vesicle
E_E	Energy cost of extracting a vesicle to the environment
E_S	Energy cost of synthesis of a messenger molecule
E_V	Energy cost of producing a vesicle to carry messenger molecules
Env	Environment
h	Distance between two adjacent transmitter bio-nanomachines
I_p	Regularized incomplete beta function
$I(X;Y)$	Mutual information
K_b	Boltzmann constant
n_{aa}	Number of amino-acids in the messenger molecule
N_c	Number of molecules received at the receiver in a symbol duration, belonging to the current symbol
$N_{c(i)}$	Number of molecules received at the receiver in a symbol duration, belonging to the current symbol with i number of molecule release
N_{hit}	Total number of molecules received at the receiver in a symbol duration
n_i	Average number of molecules released for a single symbol when the bit value of the symbol is i
n_{max}	Maximum number of molecules that can be produced with the given energy budget

N_n	Number of molecules received at the receiver in a symbol duration, belonging to noise
N_p	Number of molecules received at the receiver in a symbol duration, belonging to the previous symbol
$N_{p(i)}$	Number of molecules received at the receiver in a symbol duration, belonging to the previous symbol with i number of molecule release
n_s	Positive integer between 1 and n_{max}
n_t	Number of concurrent independent channels, sent from the transmitter
$P(\alpha)$	The distance a molecule has to traverse from the transmitter to the receiver
P_{hit}	Probability to hit
P_{hit}^R	Probability to hit to the correct receiver, in case of two transmitting pair
P_{hit}^W	Probability to hit to the wrong receiver, in case of two transmitting pair
$P_{R(p,c)}$	Size of the propagating molecule
$P_{R(s_p,s_c)}$	The probability of successfully receiving the current intended symbol
$P_{R(s_p^R, s_p^W, s_c^R, s_c^W)}$	Successful reception probability of s_c^R
$P_{X_j(s_p,s_c)}$	The probability of incorrectly decoding the current symbol s_c as j
$P_{X_j(s_p^R, s_p^W, s_c^R, s_c^W)}$	Incorrect decoding probability of s_c^R as "j"
Pw_B	Power used for routine background activities
Pw_C	Power available for communication purposes
Pw_T	Total power produced by a bio-nanomachine
$r_{affinity}$	Affinity radius of a receptor
r_{cell}	Radius of a bio-nanomachine
$r_{effective}$	Effective radius of a bio-nanomachine
r_{mm}	Radius of a messenger molecule
r_s	Stokes' radius of the propagating molecule
r_{tx}	Radius of the transmitter bio-nanomachine

r_v	Radius of a vesicle
$Q(.)$	Tail probability of standard normal distribution
s_c	Bit value of the current symbol
s_p	Bit value of the previous symbol
s_{pm}	Size of the propagating molecule
s_{fluid}	Size of the molecules of the fluid
T	Temperature of the environment
t_s	Symbol duration
T_m	Type of the messenger molecule
α	The angle between the two following lines; the line between the release point and the center of the transmitter and the line between the centers of the transmitter and the receiver
β	Release point angle at which the straight line between the centers of the molecule and the transmitter is perpendicular to the straight line between the centers of the molecule and the receiver
δt	Step time
η	Viscosity of the fluid in the environment
τ	Threshold value for bit value evaluation
τ^*	Ideal threshold value
τ_{S_p}	Threshold value for bit value evaluation when the previous symbol is s_p
τ_{S_pI}	Threshold value for bit value I's evaluation when the previous symbol is s_p

LIST OF ACRONYMS/ABBREVIATIONS

ACI	Adjacent Channel Interference
ADP	Adenosine diphosphate
AGWN	Additive Gaussian White Noise
ASK	Amplitude Shift Keying
ATP	Adenosine Triphosphate
BCSK	Binary Concentration Shift Keying
BMoSK	Binary Molecular Shift Keying
CNT	Carbon Nano Tubes
CCI	Co-channel Interference
CICR	Calcium Induced Calcium Release
CS	Calcium Signaling
CSK	Concentration Shift Keying
CvD	Communication via Diffusion
ER	Endoplasmic reticulum
FSK	Frequency Shift Keying
HCP	Hexagonal Close-Packed
ISI	Intersymbol Interference
ICW	Intercellular Calcium Waves
IP_3R	IP_3 Receptors
MC	Molecular Communication
MNT	Molecular Nanotechnology
MEMS	Microelectromechanical Systems
MoSK	Molecular Shift Keying
MTOC	Microtubule Organizing center
NEMS	Nanoelectromechanical Systems
PLC	Phospholipase C
PKC	Protein kinase C
PPM	Pulse Position Modulation

QCSK	Quadruple Concentration Shift Keying
QMoSK	Quadruple Molecular Shift Keying
SNR	Signal-to-noise Ratio
UWB	Ultra Wide Band

1. INTRODUCTION

The first half of the 20th century has been filled with events of huge scale, incomparable to the ones in the whole past history. While on the one hand there were events that caused great sorrow and misery, at the same time by the efforts of remarkable and visionary man and woman great scientific breakthroughs have been achieved that shaped all the societies of the world.

One of these breakthroughs is undoubtedly, the invention of the transistor. The production of the first silicon-based transistor by Texas Instruments in 1954 heralded the coming age of electronics. Five years later the world-renowned theoretical physicist Richard Feynmann, gave his well-known speech called "There's plenty of room at the bottom" [3]. In this speech, he mentioned that according to the physics knowledge of 1959, construction of objects in nanoscale is possible and they can have unsurpassed capacity and capabilities. He urged the scientific community to pursue research in building machines and storing information in nanoscale. This has been the first world-wide mentioning of nano-scale research and nano machines. Following this vision, scientists and researchers pushed forward in this so-called miniaturization effort with the goal of building smaller and smaller electronic chips. In 1965, Gordon E. Moore published his well-known Moore's Law [4]. This law predicted that the number of transistors that can be placed on an integrated circuit will be doubled in every two years and this law proved to be correct for the last 40 years.

In 1974, Norio Taniguchi coined the term Nanotechnology in his paper [5] for the first time. Yet, the promotion of this novel idea to its current popularity had to wait till 1986 with Eric Drexler's book "Engines of Creation: The Coming Era of Nanotechnology" [6]. In his book, Drexler described in detail how nanomachines can be built, their properties and capabilities, the design challenges in the nanoscale, and what kind of applications nanomachines will offer for the daily life. He also hypothesized "the universal assembler" devices, which can build other machines (including themselves) atom by atom.

Lately, microprocessor technology favors parallelization technologies in order to increase the processing power in contrast to further miniaturization as the last few decades. Thus, it seems using the current integrated circuit manufacturing technology, the limit to Moore's Law has been met. While the current technology enables the production of 15 to 22 nm-sized transistors inexpensively, the resulting microprocessors are in the scale of millimeters. In order to advance further in the miniaturization endeavor, newer manufacturing techniques such as finer photolithography and novel components (e.g. carbon nanotubes), are required. These methods seem to enable the production of entire processors within 0.1 to 1 μm scale. These Nanomachines, with their extremely small sizes, will enable the development of new applications in various fields such as nanomedicine, nanotechnology-on-a-chip (i.e., nm-sized lab-on-a-chip systems), and tissue engineering [7, 8].

1.1. Nanomachines

Currently, there are three different approaches for the realization of these nanomachines. The top-down approach emphasizes the use of larger machines to build smaller machines. In contrast, the bottom-up approach focuses on building nanomachines from even smaller objects, namely molecules and atoms. The last approach, bio-mimicking or bio-nanotechnology, targets the use of living organism cells as a baseline for nanomachine development.

1.1.1. Top-down approach

Initially mentioned by the Foresight Institute in 1989, this traditional approach aims to build nanomachines by using special higher scale tools (e.g. optical or electron based lithography tools). The main idea in this approach is the use of larger machines to build smaller machines. Though not a strict definition, nanomachines built by this approach are called Nanoelectromechanical Systems (NEMS) following the tradition of Microelectromechanical Systems (MEMS).

The use of a direct manufacturing tool enables the manufacturer to have high

level control over the design of the nanomachine. Currently, most of the research in this approach utilizes a very versatile nanomaterial called Carbon Nano Tube (CNT) as the building block. The unique properties of CNTs (e.g. its ability to act like a 1D object instead of a 3D object) make them applicable to the nanoscale machinery manufacturing. Nanotubes can also be used as transistors for the electrical circuits of NEMS.

Nonetheless, the resolution of today's manufacturing tools limit the size of a nanomachine built by this approach. Also, the physical properties of the nanoscale environment makes direct miniaturization attempts inapplicable in most cases. Thus, the traditional machinery manufacturing processes must be revised for the nanoscale environment's physical properties before being applied to the nanoscale. Even though they present appropriate solutions for NEMS, there is an important problem when they are used in a real-life environment. Their carbon based structure reacts with oxygen that changes their chemical properties and makes it unusable in such environments. Since in a real-life environment there is abundant amount of oxygen available, this problem currently limits the applicability of CNT-based NEMS designs to lab environments.

1.1.2. Bottom-up approach

The second important approach for building nanomachines is the bottom-up approach. This approach envisions molecules building nanomachines themselves. An extreme scenario based on this approach is the aforementioned Universal Assembler idea. In this scenario, nanomachines are designed and built atom-by-atom. Due to their chemical properties, certain chemical bonds are formed between certain molecule pairs when they come into close contact. This approach utilizes these chemical properties and uses them in nanomachine manufacturing. Another name used for this approach is Molecular Nanotechnology (MNT); the nanomachines built by this approach are called molecular nanomachines. In the literature there is also a subdivision of this approach, called DNA nanotechnology. This subdivision aims building nanomachines from DNAs instead of molecules. DNA's versatility to form different structures out of its strands are being used in this method.

Instead of going against nanoscale dynamics and trying to find workarounds to overcome them, this approach utilizes nano-scale dynamics in the process of building the machines. Because of this building process, nanomachines built with this approach are finer in scale compared to the nanomachines built by the top-down approach. Also, the absence of higher scale specialized tools to build the nanomachines enables them to self-replicate and self-repair.

On the downside, this self-building process limits the manufacturer's control over the end product nanomachine. Also, there may not be any appropriate chemical bonding available for a desired nanomachine. Currently, only very simple structures can be built from molecules. Further research is necessary for building bigger, more complex nanomachines with this method.

1.1.3. Bio-mimicking approach

All living organisms are composed of trillions of nanoscale components called "Cells". They have a wide variety of capabilities. To enumerate a few: they can sense the environment, give response based on external stimuli, store information, communicate with each other, generate mechanical energy by using chemical energy. Most of these capabilities are also expected from nanomachines, so, capability-wise, cells are similar to what is envisioned for nanomachines. Instead of designing nanomachines based on our micro- or macro-scale machinery knowledge, nanomachines can be designed based on cells. A variant of this approach is to bio-engineer cells to perform the tasks that we program. These ideas form the basis of this bio-mimicking approach and is also called Bio-nanotechnology [9]. The nanomachines constructed following this method are also called bio-nanomachines.

Since cells are already working in the nanoscale, their design principles are appropriate to nanoscale dynamics. Therefore, we can directly apply methods learned from cells to nanomachines. Also, cells have capabilities like self-replication and self-repairing; nanomachines based on this approach can also have these features, which increase the usefulness of these devices.

The main challenge in this approach is quite different than the previous methods. In order to emulate cell behavior, first we have to understand how the cells work and discover how to bio-engineer some desired behaviors. Currently, the general workings of cells are known, but the details of specific mechanisms need further research.

1.1.4. Features of nanomachines

The target use of nanomachines covers a wide spectrum of applications and environments. The features that should be supported by nanomachines can be classified in two categories:

- *Traditional features*: Features supported by higher scale machines (e.g., sensing the environment, communicating among nanomachines and between the nanomachine and external higher scale environment, manipulating objects around the machine, reliability, computational capability, mobility, and energy efficiency)
- *Nano-scale features*: Features unique to the nano-scale and features necessary in the nano-scale environment (e.g., nano-scale size, self-replication and/or self-assembly, self-repairing, low-power consumption, and self-sustainability)

The first and most significant feature of a nanomachine is its small size. Due to its size, a nanomachine is able to operate in places where higher scale machines cannot. This feature is especially very important in some environments. The foremost example of these environments is inside the living organisms. A single nanomachine or a cluster of nanomachines can easily enter inside a living creature and perform tasks within. After initial deployment, deploying additional nanomachines to replace faulty and inactive nanomachines is a difficult process. The self-assembly and self-replication capabilities of the bottom-up and the bio-mimicking approaches increase the lifetime of a nanomachine system and greatly reduce the need for such re-deployments. Nanomachines are expected to have very limited energy storage capabilities. They have to be both energy efficient and self-sustainable. Cells are very successful in energy efficiency. The mechanical systems inside cells (i.e., molecular motors) are many times more energy efficient than macro-scale machines. These methods can be mimicked for building

energy efficient mechanical systems. Nanomachines can also have computational capabilities comparable to small computers. In [10], several theoretical models show that it is possible to develop a Turing machine via DNA strands and appropriate enzymes. However, in order to attain significant amounts of computational power, nanomachines should be able to communicate with each other.

1.1.5. Applications for Nanomachines

Nanomachines can be used in a wide variety of applications where manipulation on the nano-scale is either necessary for the application or greatly increases the effectiveness of the application. They can be used as tools, sensors, processors, and information storage units in the nano-scale. In the literature, most of the initial applications of nanomachines are expected to be in the medical field. Due to their extremely small size, nanomachines can enter and work from the inside of living organisms where larger scale machines either cannot work or can only work in a very crude sense. This capability enables the development of many applications using nanomachines. Examples for these medical applications are as below.

- *Health monitoring*: Diagnosis is a crucial part of a treatment procedure. Nanomachines, placed near critical parts of the body, can act as a diagnosis tool. They can sense and report the conditions of nearby body parts. In case of an illness or disease, the medical examiner first checks these logs to understand the current and past conditions of the patients body instead of running numerous test trials.
- *Nanomedicine*: In case of drug distribution within a living organism, some drugs should be targeted to a specific cell tissue. Other cell tissues can be adversely affected by these drugs. Nanomachines can be used to seek these specific cell tissues and deliver the chosen drug only to the targeted cells while ignoring other types of cells.
- *Immunization system augmentation*: Nanomachines can easily sense the presence of any microorganisms, viruses, and toxins in the environment. If this sensing capability is combined with taking action to eliminate those unwanted objects, a defense system against harmful microorganisms and materials can be built.

Injected inside living organisms, such defense systems can act as an additional line of defense against foreign microorganisms and materials.

- *Interfacing with prosthetics*: Future prosthetics are expected to be based on robotic appendages. In order to fully coordinate their use, prosthetics should interface with the rest of the body (especially the central nervous system). Nanomachines can fill this gap between the robotic prosthetics and the organic nervous and muscular systems by relaying and converting information for a better or complete coordination of the substitute appendages.

Beyond medical applications, various applications can be developed using nanomachines such as intelligent, self-maintaining and self-repairing materials, human augmentation, environmental monitoring, intelligent green energy systems.

1.2. Nanonetworking

Regardless of the utilized approach, a single nanomachine is expected to be too simple to perform complex functions, especially if this function is one that has macro scale results. Nanomachines should be able to work together with other nanomachines to perform such complex functions. Clusters or groups of nanomachines are expected to be developed for applications that utilize such complex, higher functions. Nanorobots, a group of nanomachines working together, and nanoclouds, nanomachine colonies with thousands or even millions of nanomachines, are a few theorized examples of such clusters. The key element in these kinds of clusters is the communication ability of the nanomachines among themselves. We call this communication paradigm as the "Nano-scale Communication" or "Nanonetworking".

While some researchers consider extending traditional systems to this new domain (e.g. wireless communication in the terahertz band [11]), others try to build novel systems based on biological intra- and inter-cellular communication methods found practically in all living things from prokaryotes, single-celled organisms, to highly advanced multicellular ones, such as humans. Some examples of these biological communication systems are the stimulation of skeletal muscle fibers by motor neurons at the neuro-

muscular junction, Intercellular Calcium Waves (ICW) coordinating group behavior in astrocytes, and wire-like microtubular structures carrying hard to diffuse intracellular components in the cytosol [1]. Following these systems and many others, researchers have been proposing different systems, commonly called Molecular Communication (MC) systems in the literature. Recently, IEEE has started a new working group, "IEEE 1906.1 Recommended Practice for Nanoscale and Molecular Communication Framework" focusing on these issues.

1.3. Traditional methods for nanonetworking

Several traditional communication methods are proposed for nano-scale communication. They are usually based on communication systems that are in use in micro and macro-scale.

1.3.1. Electromagnetic communication

Electromagnetic waves considered for communication between nanomachines are comprised of low-to-medium frequency and high-to-extremely high frequency waves. Low-to-medium frequency waves can pass through many materials including living tissue easily which makes them applicable to various environments. However, generating electromagnetic waves at this frequency from a nano-scale antenna requires high amounts of energy, and the resulting signal carries very little amount of information to be useful at the receiving end. The main reason of this problem is the wavelength used in the transmission. The antenna size of an electromagnetic wave transmitter should be at least a substantial fraction of the size of the wavelength of the waves. Due to its size, a low-to-medium frequency nanoscale transmitter needs enormous amount of energy to transmit signals. On the other hand, this kind of communication can be used to send data in the downlink from micro- or macro-scale machines to nanomachines. The average energy budget of micro- and macro-machines are appropriate for low-to-medium frequency wave generation and nanoscale antennas can easily detect and decode these signals [8].

High-to-extremely high frequency signals have a higher absorption rate from materials and living tissue. Also, more transmission power is needed from the transmitter compared to lower frequency signals. Yet, an electromagnetic wave at these frequencies can easily be produced with nanoscale antennas, which decreases the required transmission power. In [8], Freitas calculates that for a nanoscale machine with a 1 pW energy budget for communication, 10^6 zJ is needed to transmit a single bit. This leads to a data rate limit of 10^3 bps for such a nanomachine.

In [12], Akyildiz *et al.* propose an electromagnetic nanonetworking system using graphene based antennas capable of transmitting electromagnetic signals in terahertz frequencies. They discuss this system in the context of a nanosensor device with a size of 10 - 100 μm^2, constructed using the top-down approach. In [13], the same authors develop a channel model and power allocation patterns for this communication system. In this work, they show that there is a unique noise type called Molecular Absorption Noise in this environment. The molecules that form the environment (e.g., water molecules inside a liquid) drain some energy from the signal. This unique noise source introduces considerable path loss and makes the communication signal only viable for very short ranges (e.g., 10^{-4} meters). In their later works, the authors add the energy constraint to their channel model and show that, with a basic modulation scheme, such a system can achieve $3 - 7$ bps, even lower than Freitas's expectations [14]. The transmitter system they consider has a higher energy consumption than the rough calculation of Freitas, which can be developed further in the future. Due to the molecular absorption noise source, they propose using a pulse-based signal similar to the Ultra Wide Band (UWB) systems [15]. They also propose a MAC layer for such a system, considering a handshaking step for a pulse-based system and elaborate on a receiver architecture [16].

1.3.2. Acoustic Communication

Acoustic communication utilizes acoustic waves to transmit information. It is widely used as an underwater communication system since sound waves can easily propagate through water over long distances. Freitas has evaluated the usage of acous-

tic waves for communication between nanomachines for living organisms [8]. He states that the use of acoustic waves with frequencies between 10 and 100 MHz is ideal for this environment. It is calculated that acoustic communication can attain data rates up to 10^7 bps for distances over 10 - 100 micrometers (1 to 10 cells assuming cells of 10 μm diameter) but consumes too much power (approximately 6000 pW) for a nanomachine. These rates are expected to be worse if the environment is selected as free space since acoustic waves travel much slower in air than in water (343 m/s compared to 1482 m/s). Another limiting factor for acoustic communication for nanomachines is the antenna size [7]. Similar to electromagnetic communication, the inherent small size of any potential antenna design for nanomachines decreases the usefulness of this kind of communication.

1.3.3. Heat communication

It is argued in [8] that heat waves can also be used for communication purposes between nanomachines. In this method, the transmitter and receiver nanomachine are immersed into a heat conductive medium and the transmitter generates heat waves to transmit information to the receiver. By modulating the frequency, amplification, and phase of the heat wave, a heat signal, which carries information similar to electromagnetic and acoustic waves, is generated. However, similar to acoustic communication, this method also requires too much power to operate for a limited range; for a bit rate of 10^4 - 1 bps for 1 - 100 μm, respectively. Also, this method requires the nanomachines to work in an environment that has high heat conductivity. Such an environment also amplifies the naturally occurring heat signatures already resident in the environment, which causes noise and further decreases the bit rate.

1.4. Molecular communication

1.4.1. Communication via diffusion

In the Communication via Diffusion (CvD) system, the information is transmitted between the transmitter and receiver through the propagation of certain molecules via

diffusion [17]. These molecules are called messenger molecules and they can be chosen as a specific type of protein, peptide, DNA sequence, or other molecular structure. At the shielding layer around the receiver (i.e., cell membrane), there are receptors that form chemical bonds with messenger molecules when they are in close proximity. The formation of such a chemical bond triggers an event inside the receiver, and thus the transmission is received. A messenger molecule must have several properties to be suitable for this kind of communication. First, it must be atoxic to the components of the communication system (i.e., transmitter, receiver, and communication medium). It should also be easily manufactured by the transmitter, and its building blocks should be abundantly available in the environment where the transmitter resides.

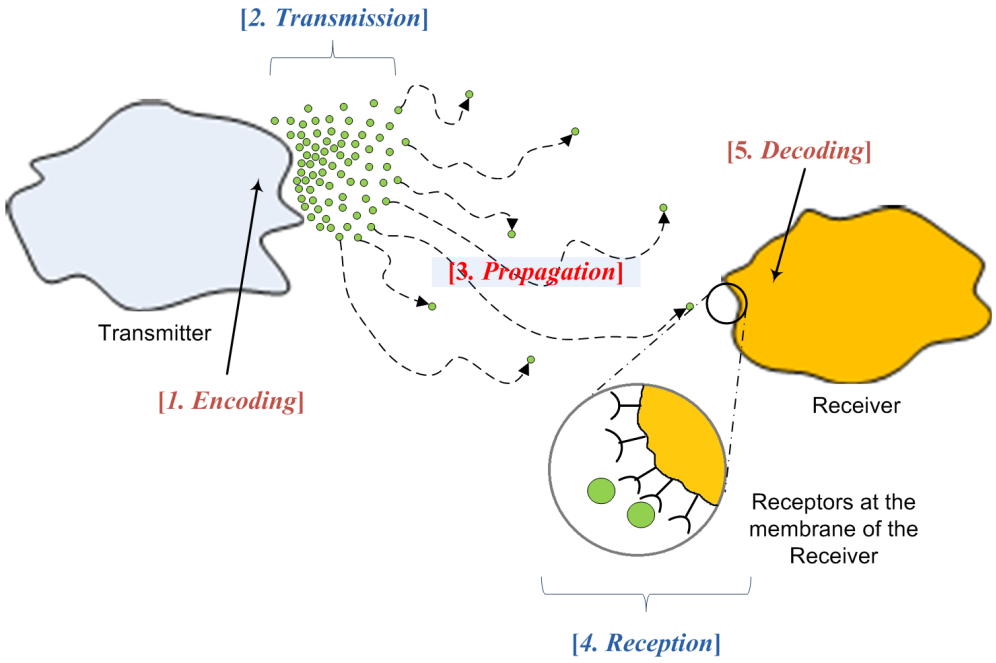

Figure 1.1. Communication via diffusion system.

In this communication system, information is sent using a sequence of symbols which are spread over sequential time slots with one symbol in each slot (Figure 1.1). The symbol sent by the transmitter is called the "intended symbol", and the symbol received at the receiver is called the "received symbol". In its most basic form, a received symbol represents one bit of information: "1" if the number of messenger molecules arriving at the receiver during a time slot exceeds a threshold, "0" otherwise. This communication system can be affected adversely from Inter Symbol Interference (ISI). Due to the diffusion dynamics, some messenger molecules may arrive after the

current time slot. Thus, the receiver incorrectly decodes the received symbol of the next time slot. This error, caused by ISI, is heavily affected by the selection of the threshold value and the time slot duration.

There are several works on the CvD system in the literature focusing on different issues. Most of these studies focus on construction a channel model, propagation dynamics of the CvD medium, and evaluating the channel capacity of the CvD system [18–22]. Other works focus on various issues such as modulation techniques, analysis of noise, synchronization, and location estimation.

The information can be encoded upon various features of the released molecule wave in this system. Llatser *et al.* formalizes the aforementioned modulation technique as a pulse-based modulation technique, and elaborate upon the effect of varying the width and delay of the pulse in [23]. Mahfuz and Chou propose using different frequencies to encode data much like the well-known Frequency Shift Keying (FSK) in electromagnetic communication [20, 24]. Due to the high delay values experienced in the propagation medium, only very low frequencies can be utilized in such a technique and even in low frequencies the resulting bit-per-second values are very low compared to other methods. We also generalize the pulse-based modulation technique as Concentration Shift Keying (CSK) and propose another modulation scheme called Molecular Shift Keying (MoSK) using different molecule representing different symbol values in [25]. These techniques will be explained in detail in Chapter 4.

In [22], the authors consider the diffusion based movement in the medium as a noise source and try to evaluate its characteristics. In a later work, they focus on the chemical properties of the ligand-receptors at the receivers and try to analyze the effects of this receiver noise [26]. Same authors also work on the encoding errors introduced to the system due to the imperfect molecular release at the transmitter [27]. They consider a transmitter design that releases the molecules in an omnidirectional fashion, from emission gaps on the cell membrane. In our work, we choose to depict the diffusion dynamics not as a noise source but the property of the channel. Also, following the biological cells' behavior in molecular release, we use a transmitter design

in which the molecules are released from a single area of the cell similar to a directional antenna compared to the omnidirectional antenna described in [28]. As explained in Chapters 3 and 6, our antenna design gives much higher channel gain compared to the omnidirectional one for a unicast transmission.

The CvD system is proposed to be used as an synchronization tool among the bio-nanomachines which utilize another system for the actual communication in [29]. Also, in [30] authors consider using beacon nodes and CvD system to find the location of a bio-nanomachine in the environment. They use this location information for addressing purposes.

1.4.2. Microtubules and Molecular Motors

Inside every cell there is a protein-based structure called cytoskeleton. This structure acts similarly to the skeleton in higher living organisms and performs many functions for the cell. One of these functions is intracellular communication via transmitting chemical structures and organelles. The part of the cytoskeleton related to this communication process is called the Microtubule. This structure starts from an organelle called centrosome and extends to the cell membrane along the cytoskeleton to form a star-like structure where the centrosome is the center (Figure 1.2). Centrosome, also called the Microtubule Organizing center (MTOC), is an organelle which is near the nucleus and acts as the center of the microtubule network. Each end of a given microtubule has a polarity value. The end near the centrosome has "-" polarity whereas the end near the cell membrane has "+" polarity. Several protein families utilize this polarity feature for movement along the microtubule; these proteins are called Motor Proteins or Molecular Motors [1].

Two of these protein families, kinesins and dyneins, utilize microtubule as a molecular rail [7] to carry objects between the nucleus and the cell membrane. They move along the microtubule by converting chemical energy into mechanical energy by the hydrolysis of Adenosine Triphosphate (ATP) into Adenosine diphosphate (ADP) (Figure 1.3). Kinesin carries its load away from the centrosome to the "+" side of the

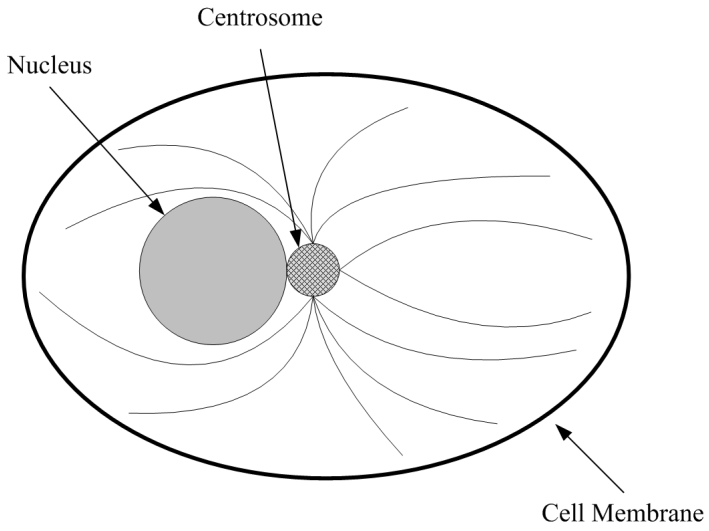

Figure 1.2. Microtubule network inside a cell.

microtubule. Dynein, on the other hand, brings objects to the center of the cell by moving towards the "-" end of the microtubule. Each of these motor proteins consists of two parts; the head and the tail parts which are attached to the microtubule and the load that is carried, respectively. These protein families (e.g. humans have 45 different kinesins) contain many members, each having the same head structure and a different tail depending on the type of the object it carries. Each member protein moves at a different speed. The fastest observed kinesin moves at a rate of 2 - 3 $\mu m/s$. Dyneins are generally faster than kinesins, the fastest observed dynein protein moves at a speed of 14 $\mu m/s$ [1].

Microtubule is a structure similar to the cables in the micro-and macro-scale communication. It allows communication along a pre defined path with little to no interference from the surrounding environment. The polarity of the microtubule and the usage of polarity-oriented motor proteins allow a unidirectional communication along the microtubule. Using these two structures, a cable-based chemical communication system can be attained. It is considerably more reliable than communication via diffusion whereas slower due to the slow movement speed of the molecular motor molecules. It can be considered as a Chemomessenger cable system. Microtubules can be used as an alternative to the carbon nanotubes in the cable-based communication for better bio-adaptability.

Several structures are proposed over the usage of the microtubule and molecular motors. In [31], Enomoto *et al.* propose the use of microtubule as a communication cable between two nanomachines. They briefly explain a network architecture using microtubules between nanomachines.

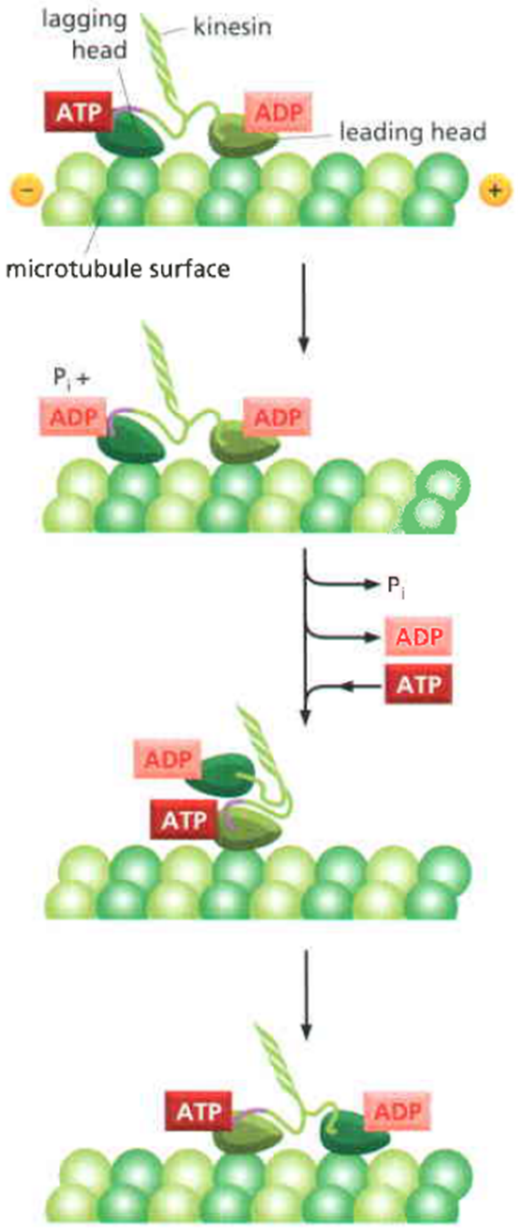

Figure 1.3. Movement over microtubule [1].

In [21], Moore *et al.* also use this microtubule based network architecture. They also describe the usage of microtubule in a hybrid propagation method of diffusion communication. In this method, each nanomachine has several microtubules extending from the nanomachine and acting like antennas. When a free-roaming molecule

attaches to one of these microtubules, the molecular motors carry them to the nanomachine, which decreases the error rate and increases the reliability of the diffusion communication. However, based on our findings such a structure increases the delay of the communication since the movement along a microtubule is slower compared to free diffusion. Also, the cytoskeleton is a dynamic structure, it is being renewed many times during the lifetime of a cell. If deployed in an extracellular environment, this turnover issue must also be taken into consideration.

1.4.3. Calcium signaling

Calcium Signaling (CS) is an alternative to the CvD system that also utilizes diffusion-based communication. In this method, the information is sent as calcium concentration change waves using secondary messengers. The information is encoded unto ion concentration waves using classical signal modulation methods such as amplitude and frequency modulation. Then, the ions diffuse inside the transmitter bio-nanomachines and pass to the neighboring bio-nanomachines until the receiver bio-nanomachine is encountered. While different types of ions such as K^+, Na^+ can be used, the most well-known and well-studied ion for this type of communication in the biology literature is Ca^{2+}.

The CS system is built based on the ICW phenomenon observed in a variety of biological tissues. Usage of ICWs in living organisms as information carriers are first noticed in the astrocyte cells, which reside in the central nervous system in animal organisms [32]. Further research revealed that various other kinds of cells (e.g. epithelial cells) also use this method for intercell communication purposes [33]. ICW is based on the relay of Ca^{2+} releasing secondary messengers; IP_3 or ATP from the stimulated cell to the neighboring cells. When a cell is triggered by one of these messengers, the endoplasmic reticulum and mitochondria of the cell releases the stored Ca^{2+} ions, which leads to a high cytosolic Ca^{2+} concentration. After some time the ions are taken back into the endoplasmic reticulum and the cell returns to its former ion concentration state. Among the two different Ca^{2+} releasing secondary messengers, IP_3 is transmitted through an internal pathway between cells while ATP is transmitted through the

extracellular environment as an external pathway using diffusion (Figure 1.4). This

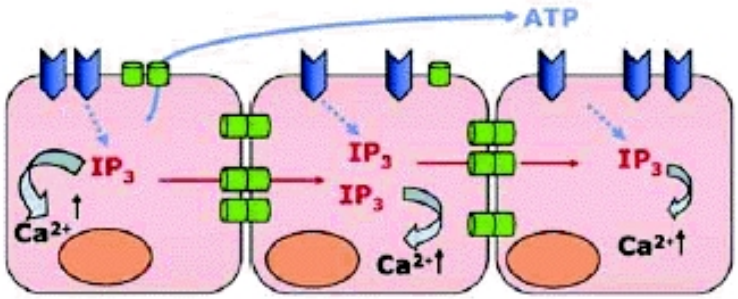

Figure 1.4. Calcium signaling and gap junctions [2].

communication system is explained in detail in Chapter 7 by giving the inner workings of ICWs and the features of the proposed communication system CS.

1.4.4. Pheromone signaling

All of the chemical communication methods explained so far, offer a solution for the short range communication between nanomachines. However, there might be cases where nanomachines are too apart from each other so that short range communication methods are ineffective due to their range limitations. Several long range communication method are described in [34] where Gine *et al.* describe the usage of pheromone, pollens, and light transducers for long range communications among nanomachines. The most notable of these methods is Pheromone Signaling.

Pheromones are widely used by animals and plants as chemical signals between different members of the same species. There are many different pheromones used for a variety of purposes. They usually propagate through the environment the species live in (e.g. air, water) via diffusion. In case of a transmission, the sender releases high amounts of pheromone to the environment. It only triggers a response at the receiver if the concentration of the pheromone in the environment exceeds a certain threshold. Gine *et al.* propose using multiple types of pheromones and classical modulation (e.g., amplitude, frequency) techniques to increase the data rate in pheromone signaling [34]. They also propose the use of special pheromone degrading enzymes to be used as a priority indicator or time-to-live parameter of the released pheromone.

The most important drawback of using pheromones as a means of communication is their high delay values. It takes seconds to minutes for the pheromones to reach at their destination based on parameters such as the distance between the sender and receiver, release concentration of the pheromone, and environmental parameters.

1.5. Contribution of this thesis

Main contributions of this thesis can be outlined as below

(i) *Joint energy and channel model*: We have developed the first joint energy and channel model for the CvD system and calculate a rough estimate of the energy cost of data transmission using this system.

(ii) *Modulation techniques*: We generalized the concentration level based modulation technique, as we call it the Concentration Shift Keying - CSK and proposed an alternative modulation technique called the Molecular Shift Keying - MoSK for the CvD system.

(iii) *Interference analysis*: We show the effects of both ISI and CCI over the performance of the CvD system and propose solutions to reduce the destructive effects of these interferences.

(iv) *Antenna design and release point selection*: We show the effects of selecting the release point of the messenger molecules over the performance of the system.

(v) *Overview of calcium signaling*: We have given an overview of the calcium signaling system and underline possible research directions and deployment schemes for this molecular communication system.

1.6. Outline of this thesis

In this thesis, we focus on one of the prominent MC systems found in the literature, called Communication via Diffusion. First, in Chapters 2 and 3 we develop a joint channel and energy model for this system considering its unique physical layer characteristics. Then, in Chapter 4 we propose two different modulation techniques to encode information on top of this molecular signal and compare their performances.

In Chapters 5 and 6, we worked on the effect of interference sources and show the importance of an antenna design in this communication system. Lastly, in Chapter 7, we elaborate on Calcium Signaling (CS), a specific version of communication via diffusion system and explain its features and propose three deployment scenarios that is suitable for this communication system. Chapter 8 concludes this thesis with giving some future directions over the research on this subject.

2. PROPAGATION AND CHANNEL MODEL FOR THE CVD SYSTEM

As stated in the previous chapter, the information is transmitted using special molecules called Messenger Molecules in the CvD system. These molecules carry the data to be transmitted between the source and the destination bio-nanomachines. The transmitter encodes the information on the messenger molecules using various properties of the messenger molecules (e.g., concentration, type, frequency) and releases them to the environment. The emitted molecules propagate in the environment via the prevalent physical dynamics in this scale (i.e., diffusion dynamics). Following this movement pattern, some of these molecules reach to the corresponding receiver and they are recognized by the special receptors at the cell membrane of the receiver. Finally, the receiver decodes the information from the messenger molecule wave. These steps constitute the three main components of a communication system: encoding, propagation, and decoding. In this thesis, we mainly focus on the propagation component of this communication system while giving a quick glance at the transmitter antenna design.

In order to analyze the propagation component of the CvD system, the first step is to build a channel model. First, we design a simple channel model using a point transmitter and a spherical receiver in a 3D free diffusion environment. In the following chapters, we introduce additional features to this model to make it more realistic while following the same principle.

2.1. Propagation Model

The most important difference of the CvD system, compared to the classical wired and wireless communication systems, is the probabilistic behavior of the medium. Due to its minuscule size, in the nano-scale, the movement of the particles inside the fluid is modeled by diffusion or in other words by the Brownian motion. This motion is

governed by the combined forces applied to the messenger molecule by the molecules of the liquid, which are in constant motion due to random thermal dynamics. In addition to this interaction, the collision dynamics between the messenger molecules should also be considered in the physical behavior. However, due to its complexity these intra messenger molecule collisions are generally not included in the literature. Moreover, it has been reported in [35] that when the number of messenger molecules in the environment is low compared to the number of molecules of the fluid, these collisions have little effect to the molecules' resulting movement pattern. Therefore, we do not consider such collisions in our model.

In a one dimensional space, the displacement of a single messenger molecule in unit time is a random variable (ΔX), which follows a normal distribution

$$\Delta X \sim N(\mu, \sigma^2) \tag{2.1}$$

where μ is taken as 0, and σ is chosen based on the selected motion type. The value of μ reflects the particle's tendency to stay still at its current position. Among the various motion types in the Brownian motion [36], we choose the free diffusion model, which is the most appropriate one for the target environment. The corresponding σ value can be calculated as

$$\sigma = \sqrt{2D\Delta t} \tag{2.2}$$

where D is the diffusion coefficient (or diffusivity) and Δt is the step time. The diffusion coefficient describes the tendency of the propagating molecules' diffusion through the fluid. It can be calculated as

$$D = \frac{K_b \cdot T}{b_{drag}} \tag{2.3}$$

where K_b is the Boltzmann constant, T is the temperature of the environment, and b_{drag} is the drag constant (or the friction coefficient) of the propagating molecule inside

the given fluid, which depends on the characteristics of both the propagating molecule and the type of the fluid. The comparative sizes between the propagating molecule s_{pm} and the molecules of the fluid s_{fluid} also affect this constant [37]. If the propagating molecule's size is similar to the size of the molecules of the fluid, it is considered as part of the fluid whereas if it is much larger, the fluid can be considered as a continuum. Based on these two different conditions, this constant is calculated as

$$b_{drag} = \begin{cases} 4\pi\eta r_s, & if s_{pm} \approx s_{fluid} \\ 6\pi\eta r_s, & if s_{pm} \gg s_{fluid} \end{cases} \tag{2.4}$$

where η defines the viscosity of the fluid and r_s defines the Stokes' radius of the propagating molecule. Stokes' radius of a molecule is different from the radius of the molecule; it is defined as the radius of a sphere whose diffusion dynamics are the same as the molecule in question in the same environment (such as fluid type and temperature). Following the discussion above, the formula of the standard deviation of this displacement becomes

$$\sigma = \begin{cases} \sqrt{\frac{K_b \cdot T}{2\pi\eta r_s}\Delta t}, & if s_{pm} \approx s_{fluid} \\ \sqrt{\frac{K_b \cdot T}{3\pi\eta r_s}\Delta t}, & if s_{pm} \gg s_{fluid}. \end{cases} \tag{2.5}$$

In our model, the particles propagate through a three dimensional environment. This movement can be modeled as three independent displacements (one for each dimension) [36] and the total displacement, $\overrightarrow{r}$, in one time step can be found as

$$\overrightarrow{r} = (\Delta x, \Delta y, \Delta z). \tag{2.6}$$

Each messenger molecule and the receiver is assumed to have spherical bodies. Whenever a messenger molecule's body coincides with the body of the receiver, the molecule is received and removed from the environment. A single messenger molecule reaches the receiver before a given deadline with a certain probability. This probability is affected mainly by the diffusion coefficient and the distance between the transmitter and the receiver.

2.2. Channel Model

Building upon the propagation model above, we quantify time as divided into equal-sized slots in which a single symbol can be sent. These time slots are called symbol durations and denoted by t_s. In the most basic setup, each symbol represents a single bit of information. The receiver differentiates between the two bit values based on the number of molecules that arrive within a symbol duration. If this number exceeds a certain threshold (denoted as τ), it decodes the symbol as "1", if not "0".

Due to the probabilistic behavior of the molecules exhibiting Brownian motion, molecules are not guaranteed to reach the receiver; instead they have a probability of hitting the receiver. This probability depends on various factors: the distance between the transmitter and the receiver (d), symbol duration (t_s), properties of the environment (Env), and the type of the molecule (T_m). The probability of hitting the receiver is denoted by $P_{hit}(d, t_s, Env, T_m)$, or $P_{hit}(d, t_s)$ for the shorthand notation, where Env and T_m are invariants. Under the assumption that each molecule propagates independently (i.e., no collision between messenger molecules), if n molecules are sent at the start of a symbol duration, the number of molecules received within the current symbol duration among these n molecules (N_c) is a random variable and follows a binomial distribution [18, 21],

$$N_c \sim B(n, P_{hit}(d, t_s)). \tag{2.7}$$

The number of molecules received in a single t_s (N_{hit}) is composed of molecules sent at the start of the current symbol duration (N_c) and at the start of all past symbol durations. As we later show in Section 2.3, only the previous symbol has a significant effect on the current symbol. N_p, the number of left over molecules belonging to the previous symbol to the current symbol duration, is also a random variable that follows the subtraction of two binomial distributions: the number of molecules received within two symbol durations and the number of molecules received within one symbol

duration.

$$N_p \sim B(n, P_{hit}(d, 2t_s)) - B(n, P_{hit}(d, t_s)) \tag{2.8}$$

A Binomial distribution, $Binomial(n, p)$, can be approximated with a normal distribution, $N(np, np(1-p))$, when p is not close to one or zero and np is sufficiently large. Therefore Equation 2.9 can be approximated as

$$\begin{aligned} N_p \quad \sim \quad & N(nP_{hit}(d, 2t_s), nP_{hit}(d, 2t_s)[1 - P_{hit}(d, 2t_s)]) \\ & -N(nP_{hit}(d, t_s), nP_{hit}(d, t_s)[1 - P_{hit}(d, t_s)]) \end{aligned} \tag{2.9}$$

As the current received symbol is only dependent on the one-bit information of the current and the previous intended symbols (s_c and s_p, respectively), in this channel model there are four different cases for received symbol decoding. The probability of successfully receiving the current intended symbol (denoted as $P_{R(s_p,s_c)}$) in this symbol duration is dependent on these cases and can be evaluated as follows.

Case ($s_p = 1, s_c = 1$): The current received symbol is both affected by the current and previous intended symbols. Since some of the molecules sent at the start of the previous symbol duration arrive late during this symbol duration, the probability of successfully receiving the current symbol as "1" increases. Thus, regarding the signal reception this is a favorable case.

$$N_{hit} \sim N(nP_2, n[P_2(1 - P_2) + 2P_1(1 - P_1)]) \tag{2.10}$$

$$\begin{aligned} P_{R(1,1)} \quad &= \quad P(N_{hit} \geq \tau) \\ &\approx \quad Q\left(\frac{\tau - nP_2}{\sqrt{n[P_2(1 - P_2) + 2P_1(1 - P_1)]}}\right) \end{aligned} \tag{2.11}$$

where $P_1 = P_{hit}(d, t_s), P_2 = P_{hit}(d, 2t_s)$, and Q(.) denotes the tail probability of the standard normal distribution.

Case ($s_p = 1, s_c = 0$): The molecules overflowing from the previous symbol duration negatively affect the successful decoding of the current intended symbol. The new symbol can be detected correctly only if the overflowing molecule count does not exceed τ. Contrary to the first case, regarding signal reception this is an unfavorable case.

$$N_{hit} \sim N(n(P_2 - P_1), n[P_2(1 - P_2) + P_1(1 - P_1)]) \tag{2.12}$$

$$\begin{aligned} P_{R(1,0)} &= P(N_{hit} < \tau) \\ &= P(N_p < \tau) \\ &\approx Q\left(\frac{\tau - n(P_2 - P_1)}{\sqrt{n[P_2(1 - P_2) + P_1(1 - P_1)]}}\right) \end{aligned} \tag{2.13}$$

where $P_1 = P_{hit}(d, t_s), P_2 = P_{hit}(d, 2t_s)$, and Q(.) denotes the tail probability of the standard normal distribution.

Case ($s_p = 0, s_c = 1$): Since the previous intended symbol contains a one-bit information of "0", there are no overflowing molecules from the previous symbol duration.

$$\begin{aligned} P_{R(0,1)} &= P(N_{hit} \geq \tau) \\ &= P(N_c \geq \tau) \\ &= \sum_{k=t}^{n} \binom{n}{k} P_1^k (1 - P_1)^{n-k} \\ &= I_{p_1}(\tau, n - \tau + 1) \end{aligned} \tag{2.14}$$

where $P_1 = P_{hit}(d, t_s)$, and $I_p(.)$ denotes regularized incomplete beta function.

Case ($s_p = 0, s_c = 0$): Since τ is always greater than zero and the current received symbol is not affected by the previous symbol, the received symbol is always equal to

zero in this case.

$$P_{R(0,0)} = 1 \tag{2.15}$$

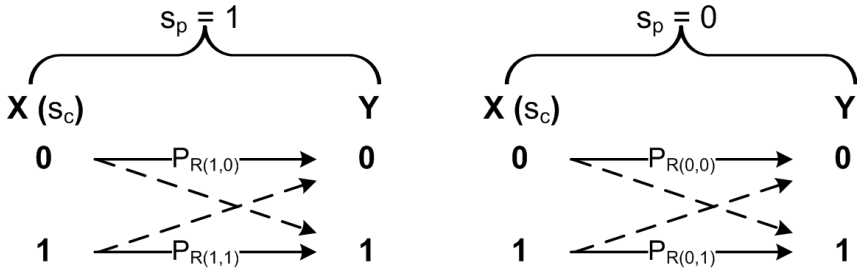

Figure 2.1. Channel model.

Considering these cases, we model the channel as a binary channel (Figure 2.1). Using this model, the channel capacity (C) can be calculated using the $P_{R(s_p,s_c)}$ values and the Bayesian rule for the marginal probabilities.

$$C = \max_{\tau} I(X;Y) \tag{2.16}$$

$$= \max_{\tau} \sum_{Y\in 0,1} \sum_{X\in 0,1} \mathbf{P}_{X,Y}(x,y) \log_2 \frac{\mathbf{P}_{X,Y}(x,y)}{\mathbf{P}_X(x)\mathbf{P}_Y(y)} \tag{2.17}$$

where $I(X;Y)$ stands for the mutual information [38, 39].

This channel capacity analysis refers to using a single type of molecule for sending the information. The throughput can be increased via the use different types of molecules, each representing a single bit of information as independent channels (molecular diversity).

2.3. Evaluation of the Channel Model

Using this channel model, we evaluate the $P_{hit}(d, t_s)$ values at various distances via Monte Carlo simulations and determine appropriate t_s values for these distances. Then, we show the effect of τ on the mutual information for different values of d and n. In this analysis, we optimize C by adjusting τ for the case $P_X(X = 0) = P_X(X = 1)$

and are equal to 0.5.

While evaluating the performance of the CvD system, we use the human insulin hormone as the messenger molecule and the molecule type specific values are selected correspondingly (e.g., Stokes' radius, r_s). The propagation environment is chosen as water at the human body temperature following the works on in vivo environments in the literature. The size of the receiver bio-nanomachine is chosen as an average eukaryotic cell. These values are given in Table 2.1. We analyze the channel capacity of the simulated communication system with different τ values.

Table 2.1. Channel model evaluation parameters.

Parameter	**Value**
Stokes' radius of insulin (r_s)	2.68 nm [40]
Radius of insulin molecule (r_{mm})	2.5 nm [8]
Viscosity of the fluid (η)	0.001 $\frac{kg}{s \cdot m}$
Temperature (T)	310 K
Boltzmann constant (K_b)	1.38 10^{23} J/K
Drag constant (b_{drag})	5.39110^{-11} $\frac{kg}{s}$
Diffusion coefficient (D)	79.4 $\frac{\mu \cdot m^2}{s}$
Radius of the receiver	10 μm [1]

We evaluate the P_{hit} values for various distances by taking a very large t_s value (30,000 s). The P_{hit} values are calculated using the number of molecules reaching at the receiver in 9000 trials. As seen in Figure 2.2, the hitting probabilities decrease exponentially with increasing distance. This behavior is due to the Brownian dynamics prevalent in the propagation of the messenger molecules.

In order to find appropriate t_s values for communication over different distances, we record the average hitting times of the molecules in the simulation. However, as seen in Table 2.2, the average hitting times for distances over 8 μm are too large and not suitable to be selected as the symbol duration of a communication system. From

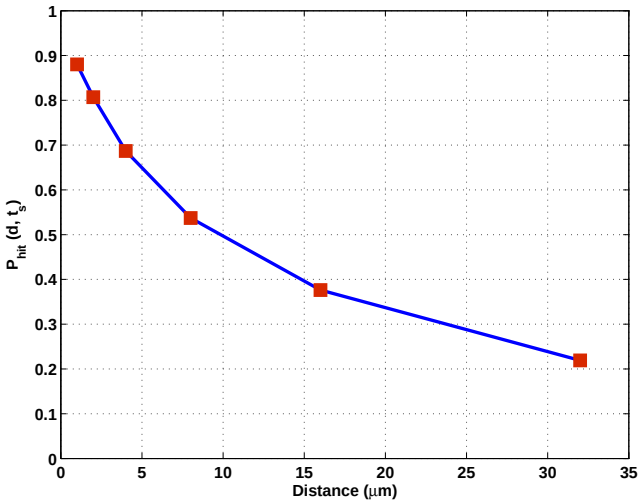

Figure 2.2. Effect of distance on P_{hit}.

the hitting time histogram in Figure 2.3, it is observed that most of the molecules arrive in a short time whereas a few molecules arrive after a very long period of time.

Table 2.2. Average hitting times.

Distance (μm)	**Average hit time (s)**
1	0.561
2	1.864
4	7.346
8	31.296
16	107.283
32	313.939

Therefore, the average hitting time values are increased to inappropriate values. Based on these histograms, we choose the t_s values as the time before which most of the molecules arrive at the receiver. For the rest of the analysis, we choose t_s values as the time before which 60% of the molecules arrive at the receiver (Table 2.3). Since different t_s values are selected for different distances we assume that before the start of the communication, the communicating pair negotiates the t_s value according to the distance between the devices.

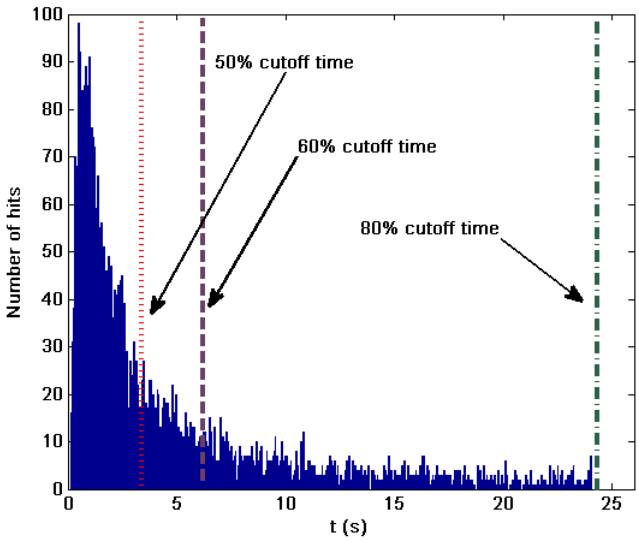

Figure 2.3. Hit time histogram cutoff at 80% (d = 16 μm). The lines refer to the time before which the mentioned percentage of hitting molecules arrived at the receiver.

After choosing suitable t_s values for different distances, we recalculate the P_{hit} values using the chosen symbol durations using 150,000 trials. In order to see the number of molecules surplus to the next couple of symbol durations, we also calculate the P_{hit} values if the symbol duration is selected as $2t_s$, $3t_s$, and $4t_s$. Figure 2.4 shows that after the second symbol duration, the rest of the molecules are spread over a wide duration. Using the t_s values selected, we calculate the channel capacities using

Table 2.3. t_s values for different distances.

Distance (μm)	t_s **(s)**
1	0.03
2	0.11
4	0.40
8	1.54
16	5.9
32	22.01

different n and τ values. Figures 2.5 and 2.6 show the effect of τ over $I(X;Y)$ where n is fixed as 100 and 500 molecules, respectively. For each distance and n couple, there

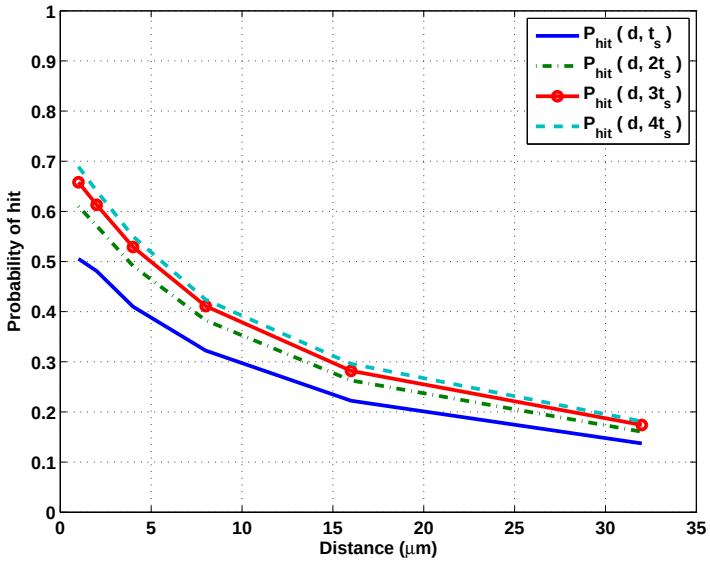

Figure 2.4. Hitting probabilities using the chosen t_s values.

is an ideal threshold value τ^*, which maximizes the mutual information rate. As seen in the figures, τ^* and C decrease as the distance increases.

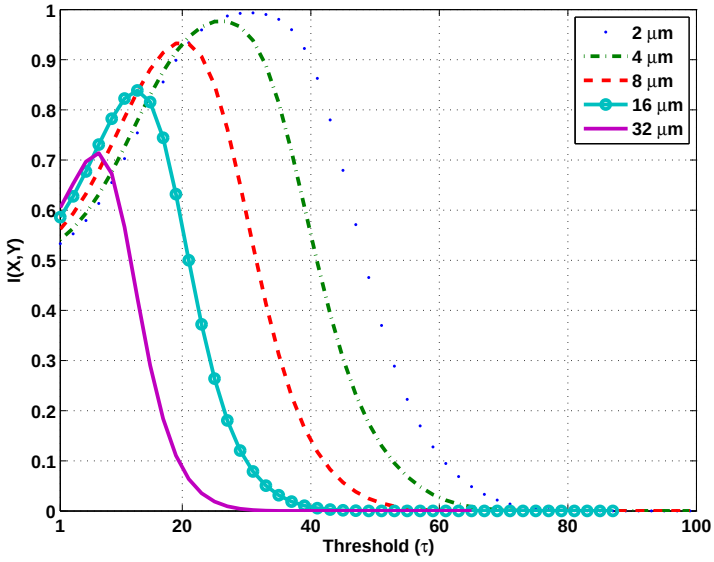

Figure 2.5. Effect of τ on mutual information (n=100).

At low τ values, after the arrival of a few molecules the receiver decides that the current symbol represents "1" whereas at high τ values, a large number of molecules should arrive at the receiver for the receiver to decode the current symbol as "1". If τ is selected as $\tau < \tau^*$, $P_{R(1,0)}$ attains a very low value and results in a low $I(X;Y)$

value since the surplus molecules from the previous symbol duration cause passing the threshold. On the other hand, if τ is selected as $\tau > \tau^*$, as the threshold value increases, at first probabilities $P_{R(0,1)}$ and $P_{R(1,1)}$ drop. After a certain threshold value, these probabilities sharply drop down to zero, since the probability of an adequate number of molecules passing the threshold decreases down to zero even with the help of the molecules surplus from the previous symbol in the case of $P_{R(1,1)}$. This behavior results in the sharp decrease of the $I(X;Y)$ values in the figures.

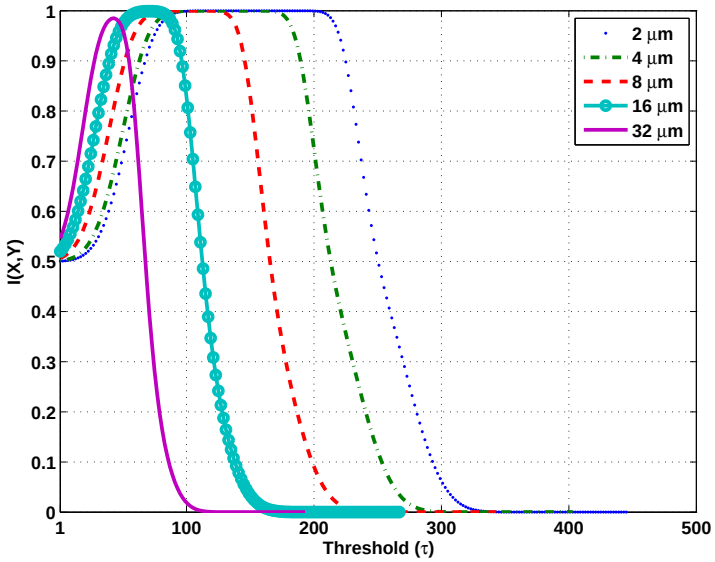

Figure 2.6. Effect of τ on mutual information (n=500).

3. ENERGY MODEL FOR THE CVD SYSTEM

In a communication system, the energy budgets of the transmitting and receiving devices introduce a serious limitation over the performance of the system. In classical wireless communication, the transmitter and the receiver have a limited battery power, which should be used efficiently by the communication system to maximize the system performance while attaining acceptable operational device lifetime values. However, in a nano- or micro-scale device, due to the size of the device, the battery can store very little energy which in turn cannot provide a long operational lifetime. In the literature, it is explained that instead of using batteries, these devices are expected to have some energy production capabilities [6–8]. Thus, energy models designed for conventional wireless systems are not suitable for this kind of communication and new models are necessary.

In this chapter, we consider systems in which each bio-nanomachine is able to produce and store energy [41]. Some of the produced energy is used by routine activities of the machine while the rest is available for communication purposes. In order to remain operational, the machine should not spend energy more than what it produces and has in its energy reserves. Also, it should not consume energy for communication purposes more than its allowance. Otherwise, it cannot provide sufficient energy for its vital systems and may become exhausted. If there is abundant energy production, the machine can store that energy for later use provided that it has available energy storage capacity. We define the total power produced by a bio-nanomachine as Pw_T, power used for routine background activities (i.e., activities for maintaining metabolic operations of the device) as Pw_B, and power available for communication purposes as Pw_C. The total power is divided into two parts as

$$Pw_T = Pw_B + Pw_C \tag{3.1}$$

3.1. Modeling energy consumption after cytosis

In a CvD system, the energy is spent for the production of the messenger molecules and their release to the environment. We model the steps of the messenger molecule production and release following the techniques used by the eukaryotic cells. In molecular cell biology, this process is known as exocytosis and is mainly composed of four steps [1] (Figure 3.1):

(i) Synthesis of the messenger molecules from their building blocks.
(ii) Production of a secretory vesicle.
(iii) Carrying the secretory vesicles to the cell membrane.
(iv) Releasing the molecules via the fusion of the vesicle and the cell membrane.

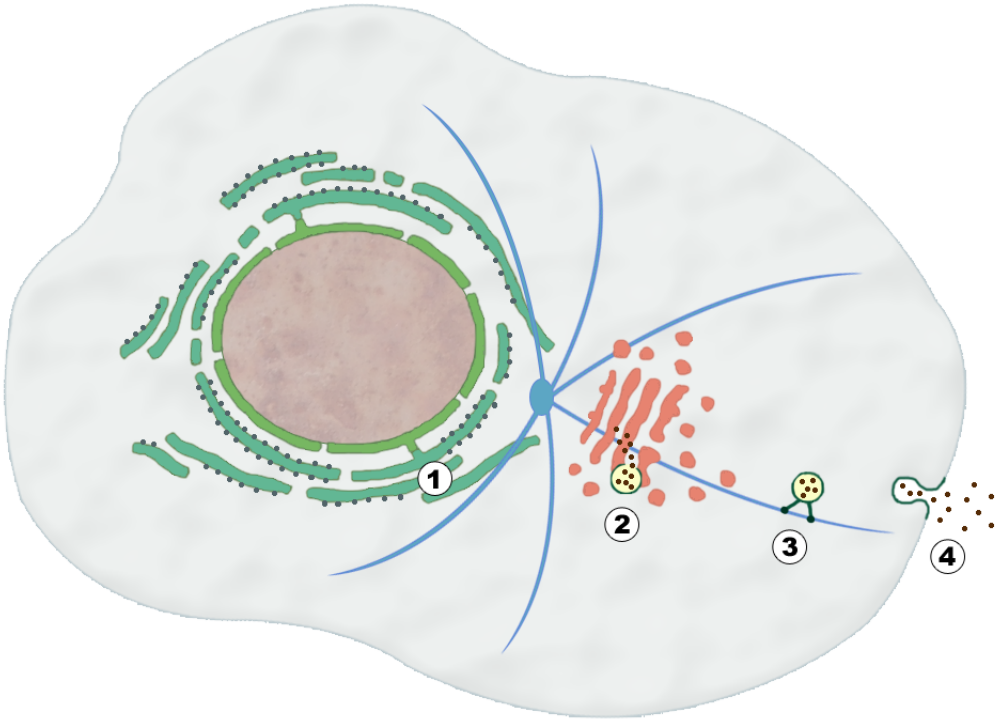

Figure 3.1. Steps of exocytosis.

The design methodology of the bio-nanomachines is a separate research issue on its own and is out of scope of this study. Regardless of its design method, we assume that a bio-nanomachine is assumed to have the following properties:

- It can generate energy from raw materials available in the environment.

- It can synthesize proteins and vesicles.
- It can synchronize with another bio-nanomachine and communicate with it using the CvD method.
- It incorporates an internal communication system similar to the microtubule in cells.
- It is wrapped inside a protective shielding layer (e.g., cell membrane) to prevent it from dissolving into the environment.

The bio-nanomachine is also assumed to have several subunits to perform these functions. These subunits are generally analogous to well known organelles of eukaryotic cells and are as follows:

- *Power Plant*: Converts raw materials to provide energy to the bio-nanomachine in a way analogous to the mitochondria.
- *Factory*: Synthesizes proteins from raw amino acids, analogous to the endoplasmic reticulum.
- *Packager*: Able to wrap several proteins or other molecules together inside a protective shell and send them to their appropriate destinations either inside or outside the bio-nanomachine, analogous to the golgi apparatus.
- *Protective Shielding*: Protects the bio-nanomachine from dissolving into the environment, analogous to the cell membrane.

A transmitting machine consumes energy in all of these steps. We define the energy cost of synthesis of a single messenger molecule as E_S, production cost of a vesicle that will carry messenger molecules as E_V, carrying cost of a vesicle as E_C, and the extraction cost of a vesicle to the environment as E_E. Vesicles are much larger in size than the messenger molecules, so each vesicle has a capacity of c_v messenger molecules[1] . Thus, if n molecules are to be sent by the transmitter, the total energy to

[1]For the sake of simplicity of the model, we assume fixed size vesicles.

be spent can be found as

$$E_T = nE_S + \left\lceil \frac{n}{c_v} \right\rceil (E_V + E_C + E_E) \tag{3.2}$$

assuming the transmitter fills each vesicle completely.

We use a protein based messenger molecule in our communication model. Proteins are synthesized at the Factory subunit by combining amino acids to form a specific amino acid chain. The number of amino acids required for a protein depends on the size of the protein. Adding a single amino acid to an amino acid chain has a fixed energy cost of 202.88 zJ [42], independent of the type of the amino acid used. Thus, the total cost to synthesize a protein that is composed of n_{aa} number of amino acids is

$$E_S = 202.88(n_{aa} - 1) \text{ zJ} \tag{3.3}$$

After the synthesis step is complete, the messenger molecules are passed to the Packager to be packed inside secretory vesicles. These vesicles are similar to the cell membrane in structure and can roughly be considered as hollow spheres whose walls are constructed out of a variety of simple structures, most notably phospolipids. The cost of synthesizing one phospholipids is 1 unit of ATP [43], which in turn equals 83 zJ [8]. In a secretory vesicle, there are 5 phospolipids in 1 nm^2 area [8]. Thus, the total cost of synthesizing a vesicle with a radius of r_v is

$$E_V = 83 \cdot 5(4\pi r_v^2) \text{ zJ} \tag{3.4}$$

Also, the capacity of the vesicle can be approximated by

$$c_v = \left(\frac{r_v}{r_{mm}\sqrt{3}} \right)^3 \tag{3.5}$$

where r_{mm} is the radius of the messenger molecule.

The vesicle moves along the microtubule from the Packager to the Protective Shielding with the help of the motor proteins. Motor proteins have two parts; one that forms a bond with the vesicle, and the other that forms two bonds with the microtubule. The motor protein releases one of its bonds with the microtubule with a process called phosphorylation, then the released part moves a single step along the microtubule and again forms the same bond with the microtubule. At each phosphorylation, the motor protein (and its load, the vesicle) travels 8 nm and spends 1 ATP of energy [1]. In a eukaryotic cell, the organelle analogous to the Packager subunit is roughly considered to be at a distance of half the cell radius fromthe cell membrane [1]. Assuming the same organizational structure in the bio-nanomachine, the overall cost of this intracell transportation is

$$E_C = 83 \cdot \left\lceil \frac{r_{tx}/2}{8} \right\rceil \text{ zJ} \tag{3.6}$$

where r_{tx} denotes the radius of the bio-nanomachine in nanometers.

At the last step, the vesicle merges with the cell membrane with a process called Membrane Fusion and the messenger molecules inside are released to the environment. After being carried to the cell membrane via molecular motors, first the vesicle docks on the cell membrane, then it is primed, and lastly the merge of vesicle and the cell membrane occurs. For a single vesicle, roughly 10 ATP of energy is consumed in this step [44].

$$E_E = 83 \cdot 10 \text{ zJ} \tag{3.7}$$

Using all of the costs explained above, the total cost to release n molecules can be written as

$$E_T = 202.88(n_{aa} - 1)n + \left\lceil \frac{n}{c_v} \right\rceil (83 \cdot 5(4\pi r_v^2) + 83 \cdot \left\lceil \frac{r_{tx}/2}{8} \right\rceil + 83 \cdot 10) \tag{3.8}$$

The number of molecules that can be produced and released in a symbol duration (n_s) is limited by the energy produced. In a long transmission, the stored energy will be depleted in a short time. Therefore, we consider the long term behavior where only the energy produced during communications is used:

$$Pw_C \cdot t_s \geq 202.88(n_{aa}-1)n + \left\lceil \frac{n}{c_v} \right\rceil (83 \cdot 5(4\pi r_v^2) + 83 \cdot \left\lceil \frac{r_{tx}/2}{8} \right\rceil + 83 \cdot 10) \quad (3.9)$$

where the units of Pw_C and t_s are zeptowatt (zW) and second, respectively; the units of r_v and r_{tx} are nm.

If n_t independent channels are used to increase the data rate, each with the same number of molecules and the same threshold value of τ, the maximum number of independent channels that can be used for a given energy budget can be calculated by using the inequality

$$Pw_C \cdot t_s \geq n_t[202.88(n_{aa}-1)n + \left\lceil \frac{n}{c_v} \right\rceil (83 \cdot 5(4\pi r_v^2) + 83 \cdot \left\lceil \frac{r_{tx}/2}{8} \right\rceil + 83 \cdot 10)]. \quad (3.10)$$

This n_t value, combined with the selected t_s and the corresponding channel capacity (C), can be used to calculate the maximum data rate of the system.

3.2. Optimization model formulation

So far we have explained the propagation, the channel, and the energy models for the CvD system. The behaviors of these models depend on several parameters. The propagation model is generally based on the environment and the type of messenger molecule. The channel model is affected by t_s, τ, d, and $P_X(X)$ values and the energy model depends on Pw_c, t_s, n_{aa}, c_v, r_v, and r_{tx}. While some of these parameters are determined by the application type (e.g., environment, d), others can be optimized to achieve better communication performance. For a communication system the maximum value of the $I(X;Y)$, which is known as C, is a definitive performance metric. We define an optimization problem that finds this C value for a single CvD channel

constrained by the communication energy budget (Pw_C) of the unit and based on the given values of d, t_s, and $P_X(X)$. Also, using C, Pw_C, and the t_s values, the maximum data rate of the system can be found by using the appropriate n_t value. We define yet another optimization problem that calculates the maximum data rate ($\frac{C \cdot n_t}{t_s}$) given a Pw_C value.

3.2.1. Maximizing mutual information

The C value can be evaluated by an optimization problem. Since we do not consider the coding aspects of the communication channel, we optimize C under given $P_X(X)$ values. Therefore, the objective function, $I(X;Y)$ depends on τ and n_s:

$$\begin{aligned} \underset{\tau,\, n_s}{\text{maximize}}\ & I(X;Y) \\ s.t.\quad n_s &\leq n_{max}(Pw_C, T_m, t_s, 1), n_s \in Z^+ \\ t_s &= \alpha_1 \\ d &= \alpha_2 \\ P_X(x=0) &= \alpha_3 \end{aligned} \tag{3.11}$$

where t_s, d, and $P_X(x=0)$ values are selected as α_1, α_2, and α_3 respectively, and n_s is a positive integer between one and the maximum number of molecules ($n_{max}(Pw_c, T_m, t_s, 1)$) that can be produced with a given energy budget. This value is a function of the power available for communication purposes, the type of the molecule, the symbol duration, and the number of independent channels. Since the number of values that can be taken by n_s and t_s is finite, this problem is solvable.

3.2.2. Maximizing data rate

Similarly, the maximum data rate ($\frac{C \cdot n_t}{t_s}$) of the system can be found by an optimization problem. The problem is similar to the one given for the mutual information maximization. However, τ and n_s have no degree of freedom. For a given n_t value, $n_s \leq \frac{n_{max}}{n_t}$, and C are evaluated by finding the optimal τ value (τ^*) as in the previous

subsection. Using this n_t, its corresponding C, and the selected t_s values, we find the data rate by multiplying C, n_t, and $\frac{1}{t_s}$. Therefore, the objective function, $(\frac{C \cdot n_t}{t_s})$, depends on n_t:

$$\begin{aligned} \underset{n_t}{\text{maximize}} \ & (\frac{C \cdot n_t}{t_s}) \\ s.t. \ \ n_s \cdot n_t &\leq n_{max}(Pw_C, T_m, t_s, n_t), n_s, n_t \in Z^+ \\ t_s &= \alpha_1 \\ d &= \alpha_2 \\ P_X(x=0) &= \alpha_3 \end{aligned} \tag{3.12}$$

where t_s, d, and $P_X(x = 0)$ values are selected as α_1, α_2, and α_3 respectively, and $n_s \cdot n_t$ is a positive integer between one and the maximum number of molecules $(n_{max}(Pw_c, T_m, t_s, n_t))$ that can be produced with a given energy budget.

3.3. Evaluation of the joint channel and energy model

Combining the channel and the energy models developed previously, and using the independent channel approach to utilize multiple molecular channels to increase the data rate of the system, we evaluate the effect of the energy budget on the communication capacity.

Table 3.1 gives the solution of the optimization problem defined in Section 3.2.1 for different distances and using various n_{max} values. In this evaluation, the c_v value is taken as 1540 and Pw_c is taken as 4.5 pW after an average pancreatic β-cell [8, 45]. As seen from the table, the capacity, C, can attain very high values at each distance after a certain n_{max} value. However, with the increase of the distance, the smallest n_{max} value that achieves high C values also increases. Since P_{hit} values for longer distances are low compared to that for shorter distances, the τ values decrease with distance. The energy budget of the bio-nanomachine allocated for communication purposes is far greater than the energy used for a single channel even when channel capacities are high (e.g., $C \geq 0.999$). This surplus energy budget can be utilized for increasing the

Table 3.1. Channel capacities for different distances and n_{max} values.

n_{max}	**2μm**		**8μm**		**32μm**	
	C	τ^*	C	τ^*	C	τ^*
10	0.642	2	0.542	1	0.322	1
50	0.935	15	0.8	9	0.603	2
100	0.993	31	0.934	20	0.713	7
500	0.999	153	0.999	103	0.985	43
1000	0.999	352	0.999	206	0.999	86

data rate by using multiple communication channels via molecular diversity. Using the optimization problem given in Section 3.2.2, we calculate the maximum data rate in terms of bps over different distances and with three Pw_C values (Figure 3.2). The reader should note that for each distance value, we use the corresponding t_s value as given in Table 2.3. We observe that as the energy budget increases, the achievable

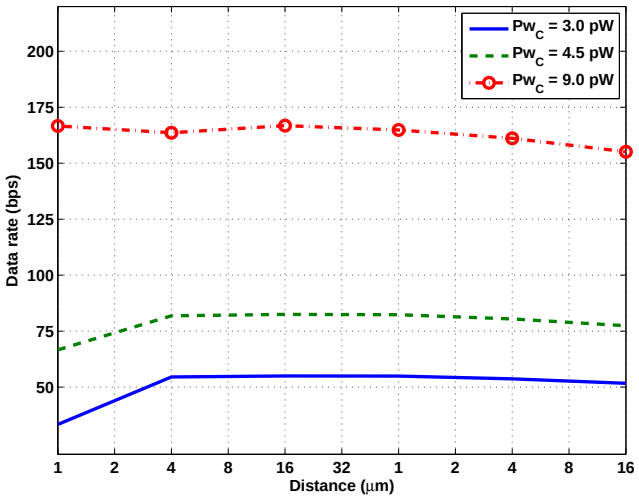

Figure 3.2. Effect of distance on data rate.

data rate increases as expected. At a distance of 1 μm, the corresponding t_s value is too low (0.03 s). Therefore, in this case $Pw_C \cdot t_s$ is very low and adequate only for small n_{max} values and few vesicles production. This vesicle production cost can be seen as a communication overhead and severely limits the usage of molecular diversity

for this distance and results in a low data rate. However, when the energy budget is high enough, as in the case when $Pw_C = 9.0\ pW$, this overhead problem is eliminated. At longer distances ($d \geq 2\mu m$), t_s values do not hinder the effective use of molecular diversity. The decrease in the P_{hit} due to distance is compensated by the increase in $Pw_C \cdot t_s$ due to the increase in t_s. Therefore, the data rate is only slightly affected by the distance.

4. MODULATION TECHNIQUES FOR THE CVD SYSTEM

In the CvD system, the information is sent using a sequence of symbols spread over sequential time slots as one symbol in each slot. As explained above, the symbol sent by the transmitter is called the "intended symbol" and the symbol received at the receiver is called the "received symbol." A variety of modulation techniques can be used for the mapping between the messenger molecule reception and the received symbol, in other words, symbol detection. The symbol can be modulated over various "messenger molecule arrival properties" at the receiver (e.g., concentration, frequency, phase, molecule type) to form a signal.

In this chapter, we propose two modulation techniques, Concentration Shift Keying (CSK) and Molecular Shift Keying (MoSK), based on the unique properties of this communication paradigm [25].

4.1. Concentration Shift Keying

This technique is the extension of the basic 1-bit modulation technique used in the previous chapters. The concentration of the received messenger molecules is used as the amplitude of the signal. The receiver decodes the intended symbol as "1" if the number of messenger molecules arriving at the receiver during a time slot exceeds a threshold (τ), "0" otherwise. In order to represent different values in symbols, the transmitter releases different number of molecules for each value the symbol can represent: for "0" the transmitter releases n_0 molecules whereas for "1", n_1 molecules are released.

CSK is analogous to the Amplitude Shift Keying (ASK) in classical communication. Instead of using two n values, (e.g., n_0 and n_1), and a single threshold, the symbol can be tailored to represent b bits by using 2^b different values with $2^b - 1$ threshold levels. We use the classical modulation naming convention based on the number of bits

per symbol. CSK can be implemented in practice as BCSK (Binary CSK) or QCSK (Quadruple CSK), depending on the bits per symbol rate.

- If b = 1, CSK is called Binary CSK (BCSK)
- If b = 2, CSK is called Quadruple CSK (QCSK)

The CvD system using CSK technique can be affected adversely from ISI, which can be caused by the surplus molecules from the previous symbols. Due to the diffusion dynamics, some messenger molecules may arrive after their intended time slot. These molecules may cause the receiver to decode the next intended symbol incorrectly. As explained in Section 2.3, in the CvD system, only the last symbol has a significant ISI effect over the current symbol. The severity of this ISI related error depends on the selection of the threshold values and the number of thresholds used in the technique given a fixed energy budget per symbol. As the the number of bits per symbol increase, the error due to ISI also increases. This is due to the fact that for higher bits per symbol value, the number of thresholds increase and this makes it harder for the receptor to correctly decoding the signal.

4.2. Molecular Shift Keying

MoSK utilizes the emission of different types of messenger molecules to represent the information. For the transmission of n information bits in one symbol, 2^n different molecules are utilized, each representing a combination of the 2^n different n-bit sequences. The transmitter releases one of these molecules based on the current intended symbol. The receiver decodes the intended symbol based on the type and the concentration of the molecule received during a time slot. If the concentration of a single molecule type exceeds the threshold, τ, at the receiver, the symbol is decoded based on the bit sequence corresponding to this molecule type. On the other hand, an error is assumed, if the concentration of any molecule types does not exceed the threshold or the concentration of more than one molecule type exceeds the threshold. Inspired by [8], Hydrofluorocarbons can be used as the messenger molecule structure for systematically designing 2^n different molecules for n-bit logical information repre-

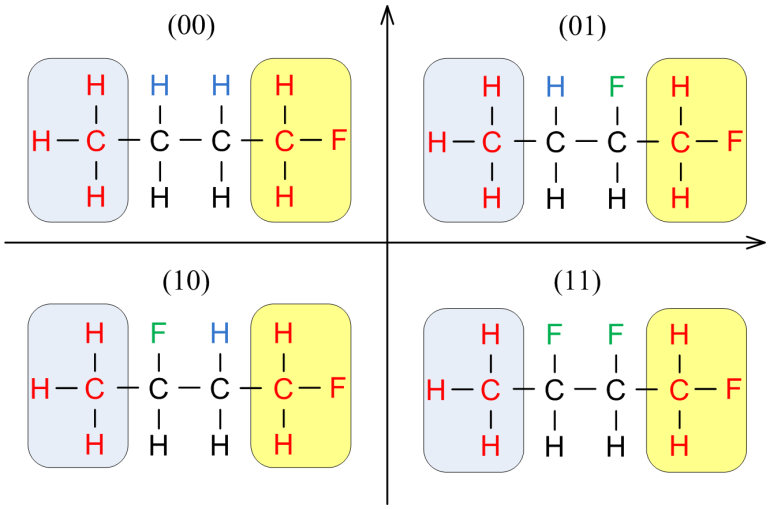

Figure 4.1. Constellation of QMoSK using Hydrofluorocarbon based messenger.

sentation [2] . Based on the message to be transmitted, a special messenger molecule is synthesized using three parts: header, trailer, and the chemical bit element. A single header and a single trailer are present in each molecule representing the start and the end of the message. For each bit of information, a chemical bit element is synthesized. This chemical bit element has two forms: one for representing "0" and another one representing "1". All of these parts are linked to each other using chemical bonds to form a single messenger molecule. In Figure 4.1, we depict a 2-bit constellation realization of this modulation technique called Quadruple MoSK (QMoSK).

Similar to the CSK technique, the surplus molecules from the previous symbols also cause ISI when MoSK technique is used. However, MoSK is less susceptible to ISI effects than the CSK technique when the bits per symbol rate (b) is greater than 1. In this case, a single threshold is used for MoSK whereas b thresholds are required for CSK. However, this advantage of the MoSK technique comes at the cost of the requirement for complex molecular mechanisms at both the transmitter and the receiver for messenger synthesis and decoding purposes, respectively. Also, a corruption in such a messenger molecule may cause some or all of the information in the symbol to get lost. This information corruption may cause severe problems since a corruption may only change the bit sequence inside the messenger molecule and the resulting corrupted molecule may still represent some information albeit not the one sent by

[2]Biocompability of such molecules is beyond the scope of this thesis

the transmitter. Without special mechanisms designed to detect (and/or correct) such errors, the receiver cannot distinguish a correct molecule from a corrupted one. In order to protect the messenger molecules from such environmental corruption, it can be sheathed inside a protective shield, e.g., vesicles, at the transmitter. When the receiver gets the vesicle, it extracts the messenger molecule inside and discards the vesicle. The design of an appropriate protective layer requires further research regarding its energy cost, protection value, and effect on diffusion dynamics.

4.3. Channel model

We modify our previous channel model according to these modulation schemes. In order to compare the two modulation schemes in terms of resilience against noise, we also add a noise source to the model. For the sake of simplicity, we model the noise source as Additive Gaussian White Noise (AGWN). Thus, in addition to the two sources that effect N_{hit}, there is a third term depicting the noise component which is a random variable following a normal distribution with zero mean and σ variance. Noise is caused by two physical elements in this system. First cause is the stray messenger molecules wandering in the environment that can attach to the receptors of the receiver. Secondly, due to environmental issues, some of the messenger molecules released from the transmitter lose their organic structure and divide into smaller parts that cannot form a chemical bond with the receiver. Thus, in effect they reduce the number of molecules reside in the environment.

$$N_n \sim Normal(0, \sigma^2) \tag{4.1}$$

Using the binomial distribution approximation to normal distribution, we can find N_{hit} as the addition of three normal distributions (N_p, N_c, and N_n).

The receiver decodes the symbol by comparing these N_{hit} values with the threshold values of the modulation technique used. In CSK technique, there are $2^b - 1$ different threshold values where b is the bits per symbol. Using these thresholds, the receiver differentiates between different bit values. The threshold values for BCSK and

QCSK implementations of the CSK technique are depicted in Figure 4.2. Since some molecules belonging to the previous symbol arrive at the receiver during the current symbol duration, different threshold values should be used based on the value of the previous symbol (S_p) to reduce erroneous decoding of the signal. Thus, in BCSK there are two threshold values whereas in QCSK there are twelve threshold values. On the other hand, in the case of MoSK techniques, a single threshold value is used both in BMoSK and QMoSK implementations. We use a binary channel model for BCSK

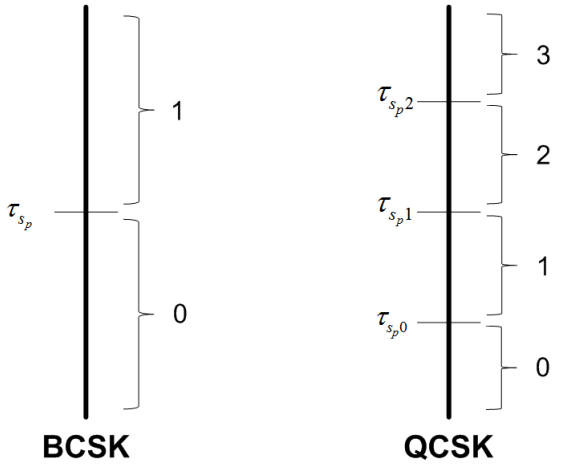

Figure 4.2. Symbol decoding for two implementations of the CSK technique ($S_p \in 0, 1$ for BCSK and $S_p \in 0, 1, 2, 3$ for QCSK).

and BMoSK implementations, and a quadruple channel model for QCSK and QMoSK implementations in order to find the successful reception and incorrect decoding probabilities (Figure 4.3). Using N_{hit} and the thresholds, these probabilities for the BCSK case can be found as follows if the current intended symbol is "0" and "1" respectively.

$$\begin{aligned} P_{R(S_p,0)} &= P(N_{p(n_{S_p})} + N_{c(n_0)} + N_n < \tau_{S_p}) \\ P_{X_1(S_p,0)} &= P(N_{p(n_{S_p})} + N_{c(n_0)} + N_n \geqslant \tau_{S_p}) \end{aligned} \tag{4.2}$$

$$\begin{aligned} P_{R(S_p,1)} &= P(N_{p(n_{S_p})} + N_{c(n_0)} + N_n \geqslant \tau_{S_p}) \\ P_{X_0(S_p,1)} &= P(N_{p(n_{S_p})} + N_{c(n_0)} + N_n < \tau_{S_p}) \end{aligned} \tag{4.3}$$

where S_p and S_c are the current and previous symbols respectively, $P_{R(S_p,S_c)}$ is the suc-

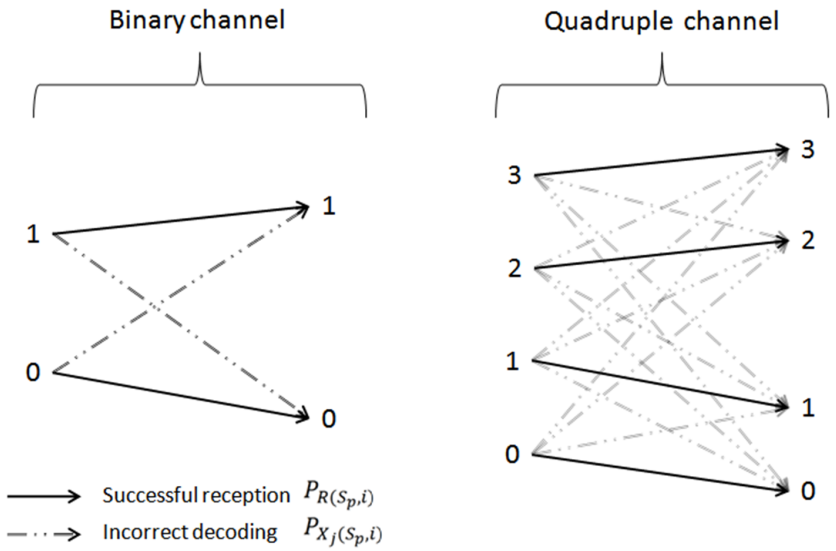

Figure 4.3. Channel models.

cessful reception probability of S_c, and $P_{X_j(S_p,S_c)}$ is the incorrect decoding probability of S_c as "j".

For the QCSK case, the successful reception probabilities are

$$\begin{aligned} P_{R(S_p,0)} &= P(a_{S_p0} < \tau_{S_p0}) \\ P_{R(S_p,1)} &= P(a_{S_p1} < \tau_{S_p1}) - P(a_{S_p1} < \tau_{S_p0}) \\ P_{R(S_p,2)} &= P(a_{S_p2} < \tau_{S_p2}) - P(a_{S_p2} < \tau_{S_p1}) \\ P_{R(S_p,3)} &= P(a_{S_p3} \geq \tau_{S_p2}) \end{aligned} \tag{4.4}$$

and the incorrect decoding probabilities are

$$\begin{aligned} P_{X_0(S_p,S_c)} &= P(a_{S_pS_c} < \tau_{S_p0}) \\ P_{X_1(S_p,S_c)} &= P(a_{S_pS_c} < \tau_{S_p1}) - P(a_{S_pS_c} < \tau_{S_p0}) \\ P_{X_2(S_p,S_c)} &= P(a_{S_pS_c} < \tau_{S_p2}) - P(a_{S_pS_c} < \tau_{S_p1}) \\ P_{X_3(S_p,S_c)} &= P(a_{S_pS_c} \geq \tau_{S_p2}) \end{aligned} \tag{4.5}$$

where $a_{S_pi} = N_{p(n_{S_p})} + N_{c(n_i)} + N_n$.

The probabilities for BMoSK and QMoSK implementations can be calculated similarly and are omitted here to avoid repetition.

Using these probabilities, we can find the mutual information, $I(X;Y)$, given the values for thresholds, distance, and the probability of hit during the current and the next symbol durations as explained in Section 2.2. By selecting ideal threshold values, the channel capacity (C) can be calculated using the maximum of mutual information as in Equation 4.6, where b stands for the bits per symbol rate used in the modulation technique.

$$\begin{aligned} C &= \max_{\tau} I(X;Y) \\ &= \max_{\tau} \sum_{Y=0}^{2^b-1} \sum_{X=0}^{2^b-1} \mathbf{P}_{X,Y}(x,y) \log_2 \frac{\mathbf{P}_{X,Y}(x,y)}{\mathbf{P}_X(x)\mathbf{P}_Y(y)} \end{aligned} \tag{4.6}$$

4.4. Performance Evaluation

We evaluate the performance of CSK and MoSK modulation techniques in terms of robustness against noise and the effect of transmission power. First, a communication system composed of a pair of transmitter and receiver, is simulated. These devices communicate with each other using the CvD system. The messenger molecule used in the system is modeled after the human insulin hormone, and the propagation environment is chosen as water. First we set the symbol duration to a very high value (t_s=36,000 seconds) and evaluate the hit times of the molecules at the receiver. Based on these hit times, we observe that after a certain duration, the hit times of the remaining molecules are widely spread over time. We choose the symbol duration (t_s) as this certain duration, rerun the simulations, and find the corresponding P_{hit} values over 150,000 trials. In order to take the ISI effect into account in the next step, the probability of hit values for single and two symbol durations are evaluated. The simulation parameters used and the resulting values are given in Table 4.1.

Using these P_{hit} values and the channel models explained in the previous section,

Table 4.1. Simulation parameters.

Parameter	**Value**
Diffusion coefficient (D)	$79.4\,\frac{\mu m^2}{s}$
Symbol duration (t_s)	$5.9\,s$
Distance between transmitter and receiver (d)	$16\,\mu m$
Probability of hit in one symbol duration ($P_{hit}(d, t_s)$)	0.2223
Probability of hit in two symbol durations ($P_{hit}(d, 2t_s)$)	0.2628

the channel capacities of BCSK, BMoSK, QCSK, and QMoSK implementations under various Signal-to-noise (SNR) values are evaluated. We use the following SNR definition: the ratio of the average received signal power to the power of the noise. The average received signal power is found by multiplying the P_{hit} values and the average number of molecules released for a single symbol (n_i). In case of the CSK techniques, since there are multiple n_i values based on the bit value of each symbol, we take the average number of molecules per symbol where the probability of a symbol having each bit value is the same. Since we use AWGN, the power of the noise is defined as the variance of the normal distribution. The conversion between the number of molecules and the resulting energy in joules, we use the energy model developed in Chapter 3.

According to the results given in Figure 4.4, all modulation techniques attain their theoretical channel capacity limits when the SNR level is high. The transmission power is defined as the number of molecules sent by the transmitter and is chosen as 1500 molecules. Since a low SNR value refers to an increase in the ratio of stray molecules in the environment compared to the actual messenger molecules released from the transmitter and as a result the incorrect decoding probability at the receiver increases. As the SNR decreases, in case of the binary implementations, BCSK offers more robustness compared to BMoSK. Since we assume the noise in the channel as AWGN, the same amount of noise is applied to both molecule types in BMoSK. Thus, BMoSK is more affected by the noise than BCSK.

In case of quadruple implementations (QCSK and QMoSK), this trend changes

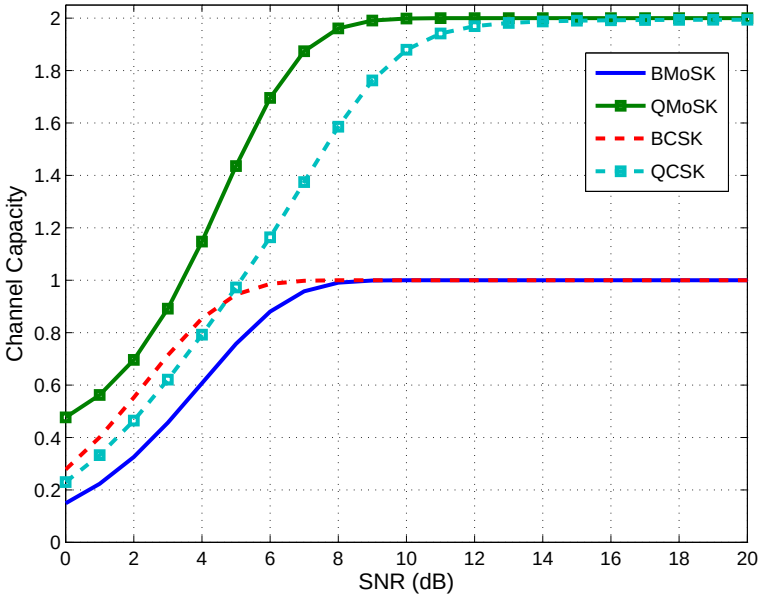

Figure 4.4. Channel capacity of different modulation techniques.

and QMoSK exhibits higher noise tolerance than QCSK. This behavior is due to the number of threshold values used in these quadruple implementations. Since QMoSK uses a single threshold value, the channel capacity can be kept high by choosing a suitable threshold value even when the noise level is high. On the other hand, in QCSK finding suitable threshold levels to keep the channel capacity becomes harder as the noise level increases. After a certain noise level (around 4 dB), the system cannot attain high successful reception probabilities regardless of the chosen threshold values. Therefore, the channel capacity drops.

The transmission power also affects the performance of the modulation techniques. As seen in Figures 4.5 and 4.6, while all modulation techniques attain high channel capacity values at high transmission power, the channel capacities decrease as the transmission power decreases. In both binary and quadruple implementations, the reduction in transmission power affects CSK techniques more than the MoSK techniques. These simulations are run with an SNR level of 20dB. In order to keep the SNR at 20dB in all simulation runs, as the transmission power increases, the variance of the noise also increases.

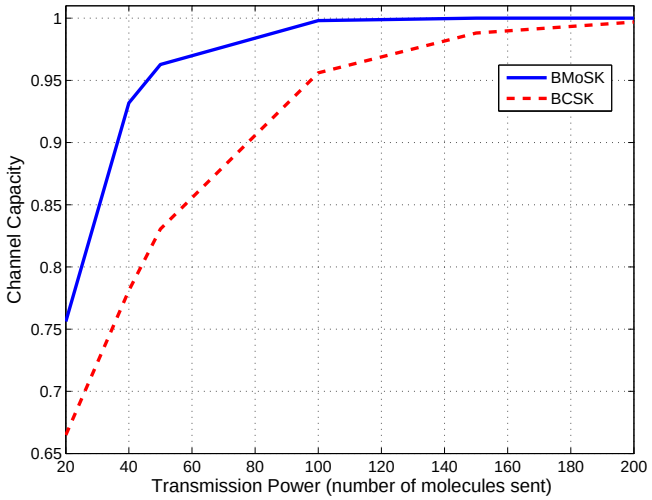

Figure 4.5. Effect of transmission power over channel capacity (Binary implementations of CSK and MoSK modulation techniques).

As the transmission power decreases, n_0 and n_1 get closer to each other. Thus, the successful reception probability of the intended symbol decreases. This behavior is

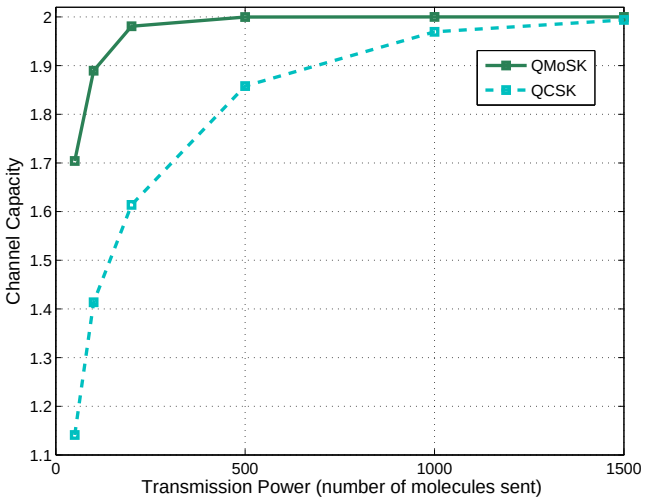

Figure 4.6. Effect of transmission power over channel capacity (Quadruple implementations of CSK and MoSK modulation techniques).

more prevalent in QCSK since four different n_i values are used instead of two in BCSK and one in both MoSK implementations. Also, as expected, regardless of the technique used, the minimum transmission power required for high channel capacities increases as the bits per symbol rate of the modulation technique increases.

5. INTERFERENCE ANALYSIS FOR THE CVD SYSTEM

In communication systems, a given signal is affected by various sources while it propagates in the medium. All elements that affect a given signal are considered as interference to the signal. These effects can either be beneficial (constructive interference) or harmful (destructive interference) to the signal in question. The most important sources of interference are the intersymbol interference (ISI), adjacent channel interference (ACI), and co-channel interference (CCI).

In any transmission, the signal is composed of a sequence of symbols, which upon aggregation, form the whole data. ISI is defined by the interference effect of a symbol onto the successor symbols. When the transmitter sends a sequence of symbols in a waveform, due to numerous reasons (e.g., multipath propagation, non-linear response from the channel), the signal representing a given symbol can affect the subsequent symbols.

ACI is the result of imperfect filtering in the transmitter, which results in the signal having some components in the adjacent frequencies. Ideally, a transmitter should only transmit the signal at a given frequency. However, due to wave forming limitations of filters, this property cannot be properly attained by a real-life transmitter circuit. Thus, a signal unavoidably causes interference to its adjacent channels.

The last major interference source, the CCI, is the effect of concurrent transmissions onto each other in a given physical environment utilizing the same frequency. When there are more than one transmitting couples in close proximity, a given transmitter's signal may also reach the other receivers. In addition to these interference sources, the signal is also affected by environmental background effects. However, these effects are not considered as a type of interference and are called noise.

We have analyzed the effects of ISI in the CvD system in Section 2.3. In this section, while retaining the ISI effects, we focus on the CCI effects in the CvD system

using both the CSK and MoSK modulation techniques described in Chapter 4 [46].

The prevalent force that affects the propagation of a signal in MC is the probabilistic behavior of the Brownian motion. While this behavior is fundamentally different from the well-known and well-studied deterministic medium of the electromagnetic wave based communication, the concept of interference still applies to MC.

As previously shown in Figure 2.3, the concentration based received signal has a log-normal like distribution in CvD. The amplitude of the signal is affected by the number of molecules released, and the variance is affected by the diffusion coefficient. Since the MC medium is inherently slow in terms of propagation delay, the symbol duration (t_s) should be selected to the left as much as possible in this distribution graph while including the spike part of the signal but leaving out some part of the long tail. However, the molecule arrival in this left out part of the tail affects the decoding process of the next symbol, and thus forms the ISI in MC. In addition to the molecules arriving at the receiver, the rest of the molecules released from the transmitter wander around in the environment and in time will be received by other devices. Considering these devices using the same type of molecule for transmission purposes, these stray molecules is the cause of the CCI effect in MC.

In electromagnetic communication, since the power of a signal diminishes with increasing range, the most common method in eliminating (or reducing) CCI among neighboring transmission couples is to utilize a reuse distance between the communicating pairs. The relationship between range and signal power also occurs in MC. Therefore, in this work we analyze the effects of the distance between two transmitters, h, over the channel capacity of the signal to see if the reuse distance method is also applicable to this communication system and show how it should be selected.

5.1. Channel model considering two transmitting pairs

In order to evaluate the effect of ISI and CCI over different modulation techniques, we alter our previous communication model. The model incorporates two communicat-

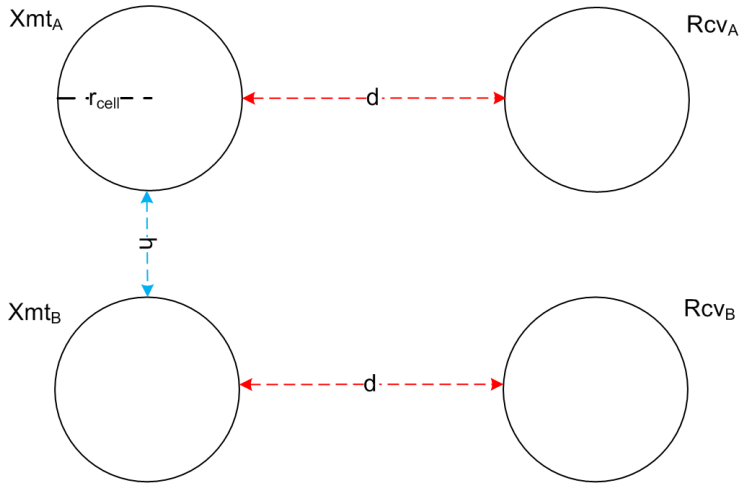

Figure 5.1. Communication model topology.

ing couples in a 3D environment, each comprised of one transmitter and one receiver bio-nanomachine. Each bio-nanomachine is modeled as a spherical body with a radius of r_{cell} and has a fixed position in the topology. In each couple, the transmitter is separated from the receiver by a distance of d micrometers. The two transmitters are placed h micrometers apart from each other, and so are the receivers (Figure 5.1).

A transmitter releases a given number of molecules depending on the bit value of the symbol (e.g., n_o for "0", and n_1 for "1"). The transmitter releases the molecules from its closest boundary with respect to the intended receiver. Hence, the release points of two cell-like nanomachines, each with a radius of r_{cell}, has a minimum distance of $2 \cdot r_{cell}$ in between due to the volume of the devices. Thus, in addition to h, r_{cell} is also an important factor for the severity of CCI since it also affects the distance between the release points of the messenger molecules.

It is assumed that the whole surface of the receiver is composed of receptors, which are able to bind with the messenger molecules. If a molecule hits a transmitter it bounces back from the transmitter since a transmitter does not have the same ligand receptors on their outer shell. The messenger molecules in this system operate in the low Reynolds number domain due to their small sizes. Thus, inertia is not a significant factor in this environment. Following this property, we model the bouncing molecule as canceling an illegal movement as if it did not happen at all [47].

Similar to the previous Monte Carlo based simulation, after finding out the appropriate t_s value, we re-run the molecule propagation trials for this duration and calculate the hitting probabilities of a single molecule to both of the receivers (P^R_{hit}, as the hitting probability at the correct receiver and P^W_{hit} as the hitting probability of the wrong receiver). Then, we calculate the distribution of the number of hitting molecules ($N^R_{c(n)}$) when a given number of molecules (n) are released from the same point at the same time as

$$N^R_{c(n)} \sim B(c(n),\, P^R_{hit}(d, t_s)). \tag{5.1}$$

In addition to the molecules originating from the transmitter, other messenger molecules may hit the receiver. Some of these molecules belong to the previous symbol of the signal while others originate from the current and previous symbols of the other transmitter. These sources act as ISI and CCI to the intended transmission, respectively. The number of molecules causing the ISI is denoted as N^R_p and follows a distribution as

$$N^R_{p(n)} \sim B(p(n),\, P^R_{hit}(d, 2t_s)) - B(p(n),\, P^R_{hit}(d, t_s)). \tag{5.2}$$

The molecules causing the CCI is denoted as $N^W_{c(n)}$ and $N^W_{p(n)}$ for molecules belonging to the current and previous symbol of the other transmitter respectively. Molecules belonging to the other transmitting pair in the environment follow similar distributions as the molecules from the main transmission as

$$N^W_{c(n)} \sim B(c(n),\, P^W_{hit}(d, t_s)) \tag{5.3}$$

and

$$N^W_{p(n)} \sim B(p(n),\, P^W_{hit}(d, 2t_s)) - B(p(n),\, P^W_{hit}(d, t_s)). \tag{5.4}$$

Combining these four molecular arrival distributions in one symbol, the total

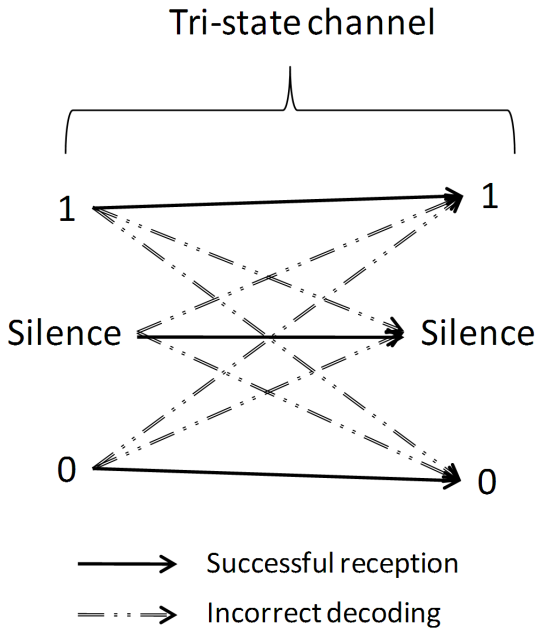

Figure 5.2. Silence Aware channel model.

number of molecules hitting the receiver in a t_s can be calculated as the summation of these sources

$$N = N^R_{c(n)} + N^R_{p(n)} + N^W_{c(n)} + N^W_{p(n)}. \tag{5.5}$$

We only utilize the binary variations of CSK and MoSK techniques (i.e., BCSK and BMoSK) for the sake of simplicity. Using a tri-state channel model that differentiates between a signal and silence (s), the symbol is decoded as silence if $N < \tau_0$, as "0" if $(N > \tau_0)\,\&\,(N < \tau_1)$, and as "1" if $(N > \tau_1)$.

Being a tri-state channel, the current symbol of the main transmission (s^R_c) and the other three symbols (previous symbol of the main transmission (s^R_p), previous symbol of the other transmission(s^W_p), and the current symbol of the other transmission (s^W_c)) can each take three values (Figure 5.2).

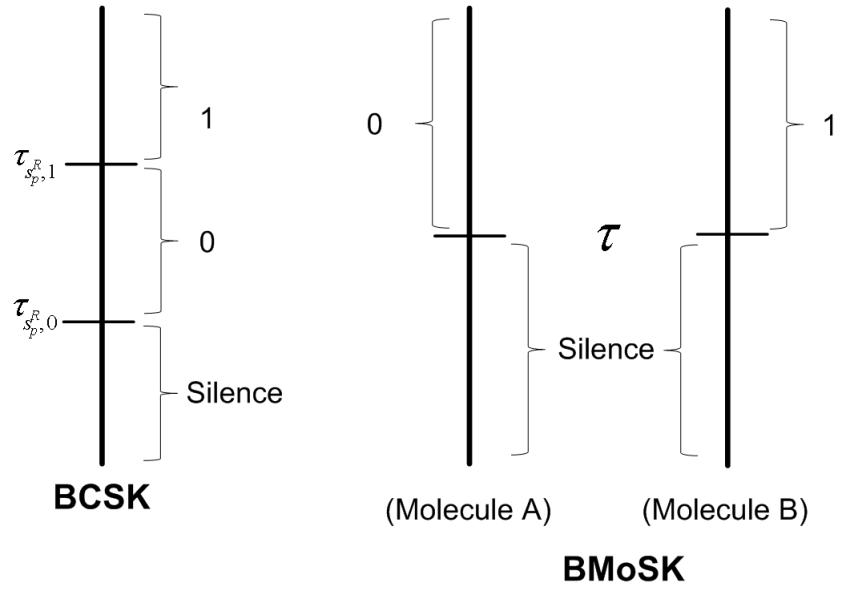

Figure 5.3. Threshold values for modulation techniques.

5.1.1. Probabilities for the BCSK Technique

Using the N value and different thresholds (Figure 5.3) for each case, the probabilities for the BCSK case can be found as follows if the current symbol (s_c^R) is "0"

$$\begin{aligned} P_{R(s_p^R, s_p^W, s_c^R=0, s_c^W)} &= P(A_0 < \tau_{s_p^R,1}) - P(A_0 < \tau_{s_p^R,0}) \\ P_{X_1(s_p^R, s_p^W, s_c^R=0, s_c^W)} &= P(A_0 > \tau_{s_p^R,1}) \\ P_{X_S(s_p^R, s_p^W, s_c^R=0, s_c^W)} &= P(A_0 < \tau_{s_p^R,0}), \end{aligned} \tag{5.6}$$

if s_c^R is "1"

$$\begin{aligned} P_{R(s_p^R, s_p^W, s_c^R=1, s_c^W)} &= P(A_1 \geqslant \tau_{s_p^R,1}) \\ P_{X_0(s_p^R, s_p^W, s_c^R=1, s_c^W)} &= P(A_1 < \tau_{s_p^R,1}) - P(A_1 < \tau_{s_p^R,0}) \\ P_{X_S(s_p^R, s_p^W, s_c^R=1, s_c^W)} &= P(A_1 < \tau_{s_p^R,0}), \end{aligned} \tag{5.7}$$

and if s_c^R is silence (s)

$$\begin{aligned} P_{R(s_p^R, s_p^W, s_c^R=s, s_c^W)} &= P(A_1 < \tau_{s_p^R,0}) \\ P_{X_0(s_p^R, s_p^W, s_c^R=s, s_c^W)} &= P(A_1 < \tau_{s_p^R,1}) - P(A_1 < \tau_{s_p^R,0}) \\ P_{X_1(s_p^R, s_p^W, s_c^R=s, s_c^W)} &= P(A_1 \geqslant \tau_{s_p^R,1}) \end{aligned} \tag{5.8}$$

where $A_i = N^R_{p(n_{s_p^R})} + N^W_{p(n_{s_p^W})} + N^R_{c(n_i)} + N^W_{c(n_{s_c^W})}$, $P_{R(s_p^R, s_p^W, s_c^R, s_c^W)}$ is the successful reception probability of s_c^R, $P_{X_j(s_p^R, s_p^W, s_c^R, s_c^W)}$ is the incorrect decoding probability of s_c^R as "j" and i is 0, if s_c^R is 0, and 1 otherwise.

5.1.2. Probabilities for the BMoSK Technique

In the BMoSK case, the probabilities are calculated considering the type of the molecules based on the bit values of the four molecular arrival sources. If the current symbol (s_c^R) is "0" or "1"

$$\begin{aligned} P_{R(s_p^R, s_p^W, s_c^R, s_c^W)} &= P(N_c^R + \delta_p^R N_p^R + \delta_p^W N_p^W + \delta_c^W N_c^W \geqslant \tau) \\ &\quad \times P(\beta_p^R N_p^R + \beta_p^W N_p^W + \beta_c^W N_c^W < \tau) \qquad (5.9) \\ P_{X_{\sim s_c^R}(s_p^R, s_p^W, s_c^R, s_c^W)} &= P(N_c^R + \delta_p^R N_p^R + \delta_p^W N_p^W + \delta_c^W N_c^W < \tau) \qquad (5.10) \\ &\quad \times P(\beta_p^R N_p^R + \beta_p^W N_p^W + \beta_c^W N_c^W \geqslant \tau) \qquad (5.11) \\ P_{X_S(s_p^R, s_p^W, s_c^R, s_c^W)} &= 1 - P_R - P_{X_{\sim s_c^R}} \end{aligned}$$

$$\delta_k^l = \begin{cases} 1, & if\ s_k^l = s_c^R \\ 0, & otherwise \end{cases} \tag{5.12}$$

$$\beta_k^l = \begin{cases} 1, & if\ s_k^l = \sim s_c^R \\ 0, & otherwise \end{cases} \tag{5.13}$$

where ($\sim s_c^R$) represents the opposite bit value of the current symbol. If the current symbol (s_c^R) is "s"

$$\begin{aligned}
P_{R(s_p^R, s_p^W, s_c^R=s, s_c^W)} &= 1 - P_{X_0} - P_{X_1} \\
P_{X_0(s_p^R, s_p^W, s_c^R=s, s_c^W)} &= P(\alpha_p^R N_p^R + \alpha_p^W N_p^W + \alpha_c^W N_c^W \geqslant \tau) \qquad (5.14) \\
&\quad \times P(\gamma_p^R N_p^R + \gamma_p^W N_p^W + \gamma_c^W N_c^W < \tau) \qquad (5.15) \\
P_{X_1(s_p^R, s_p^W, s_c^R=s, s_c^W)} &= P(\alpha N_p^R + \alpha_p^W N_p^W + \alpha_c^W N_c^W < \tau) \qquad (5.16) \\
&\quad \times P(\gamma_p^R N_p^R + \gamma_p^W N_p^W + \gamma_c^W N_c^W \geqslant \tau) \qquad (5.17)
\end{aligned}$$

$$\alpha_k^l = \begin{cases} 1, & if\ s_k^l = 0 \\ 0, & otherwise \end{cases} \qquad (5.18)$$

$$\gamma_k^l = \begin{cases} 1, & if\ s_k^l = 1 \\ 0, & otherwise \end{cases} \qquad (5.19)$$

5.1.3. Calculation of Channel Capacity

After substituting 0, 1, and s according to symbol values s_c^R, s_p^R, s_c^W, and s_p^W, the decoding probabilities and conditional channel capacities are calculated in all possible 81 cases. Summing up these conditional channel capacities with equally likely symbol values (each symbol has the same probability of being 0, 1, and s), we calculate the overall channel capacity of the system using the well-known channel capacity formulation below:

$$C = \max_{\tau} \sum_{y \in \{S,0,1\}} \sum_{x \in \{S,0,1\}} \mathbf{P}_{X,Y}(x,y)\ \log_2 \frac{\mathbf{P}_{X,Y}(x,y)}{\mathbf{P}_X(x)\mathbf{P}_Y(y)} \qquad (5.20)$$

5.1.4. Simulation Results

Based on the communication model explained above, we evaluate the effect of CCI in the CvD system with respect to different h values over two performance metrics, the probability of hitting to the receivers and the overall channel capacity. Again, we run the simulations assuming a water-like environment at average body temperature with insulin hormone-sized messenger molecules. For an acceptable ¡precision in calculation, we choose the step time in the diffusion model as 0.001 seconds. We use the average number of molecules emitted for each symbol $(n_0 + n_1)/2$ as the transmitter power, following our energy model in Chapter 3. These simulation parameters are given in Table 5.1.

Table 5.1. Simulation parameters.

Parameter	**Value**
Radius of messenger molecule ($r_{molecule}$)	2.5 nm
Diffusion coefficient (D)	79.4 $\frac{\mu m^2}{s}$
Step time (Δt)	0.001 s
Symbol duration (t_s) for $d = 4\mu m$	0.213 s
Symbol duration (t_s) for $d = 8\mu m$	0.949 s
Symbol duration (t_s) for $d = 16\mu m$	4.064 s
Symbol duration (t_s) for $d = 32\mu m$	17.391 s

First, we analyze the effect of h parameter over the hitting probabilities for different d values while setting r_{cell} to a moderate value ($5\,\mu m$). As seen in Figure 5.4, with the increase in h, P_{hit}^{W} decreases and eventually converges to zero while P_{hit}^{R} increases only slightly. Compliant to our previous works and other findings in the literature, P_{hit}^{R} decreases with increasing transmission range (d). However, P_{hit}^{W} does not show the same behavior. This is due to the fact that, when $d = 4\,\mu m$, the molecules have little space to move and most of them either hit the correct receiver or dissipate in the environment. When d increases, the molecules move more freely in the environment and they have a higher chance of hitting the wrong receiver albeit the detrimental effect of increased range. As d further increases, both hitting probabilities decrease since the

transmission range becomes the prevalent factor affecting the hitting probabilities.

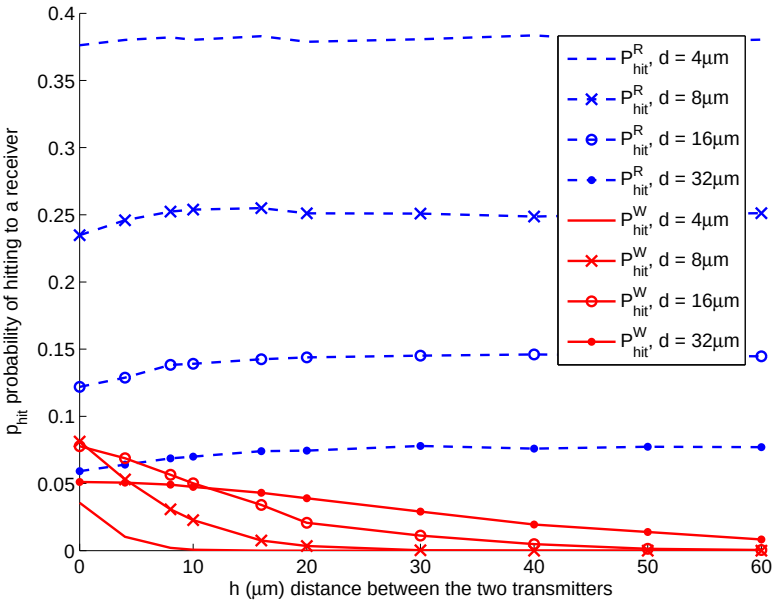

Figure 5.4. Effect of h over the hitting probabilities with varying d.

Using these hitting probabilities, in Figures 5.5 and 5.6 we depict the channel capacities with varying h and d values for both modulation techniques while the average transmission power per symbol is 333 molecules (i.e., $n_0 = 300$ and $n_1 = 700$ in BCSK, $n = 500$ in BMoSK).

For both modulation techniques, when $d = 4\mu m$, the low P^W_{hit} values do not affect the overall channel capacity. Thus, increasing h has little benefit to the system. However, as d increases, CCI starts to affect the performance of the system, and increasing h becomes a good solution to mitigate CCI as in the electromagnetic wave-based wireless communication case. As the d value increases, the difference in channel capacity between BCSK and BMoSK techniques also increases. This is due to the fact that different bit values in the environment do not affect the channel in BMoSK since a different type of molecule is used for each bit value. On the other hand, in the BCSK case regardless of the bit value, each transmission causes CCI to the other. Similar to the ISI case as depicted in Section 4.4, BMoSK is also more resilient to CCI. Next, we set the transmission range as $16\,\mu m$ and analyze the hitting probabilities for different r_{cell} values.

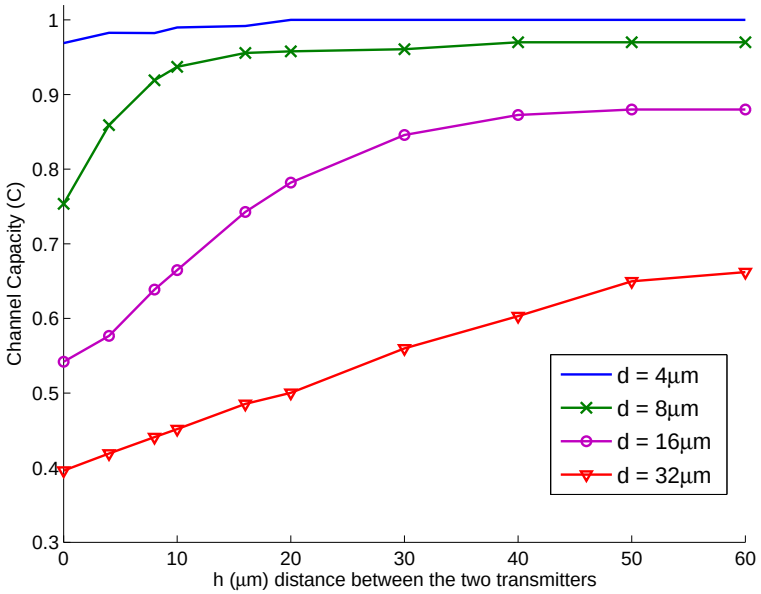

Figure 5.5. Effect of h over Channel capacity with varying d using BCSK.

As seen in Figure 5.7, the cell radius heavily affects P_{hit}^{R} since hitting the receiver is proportional with the volume of the receiver in the 3D environment, and the spherical volume decreases cubically with decreasing r_{cell} value. Similar to the Figure 5.5, this behavior in P_{hit}^{R} is not reflected in the P_{hit}^{W} values. Although, the decrease in the

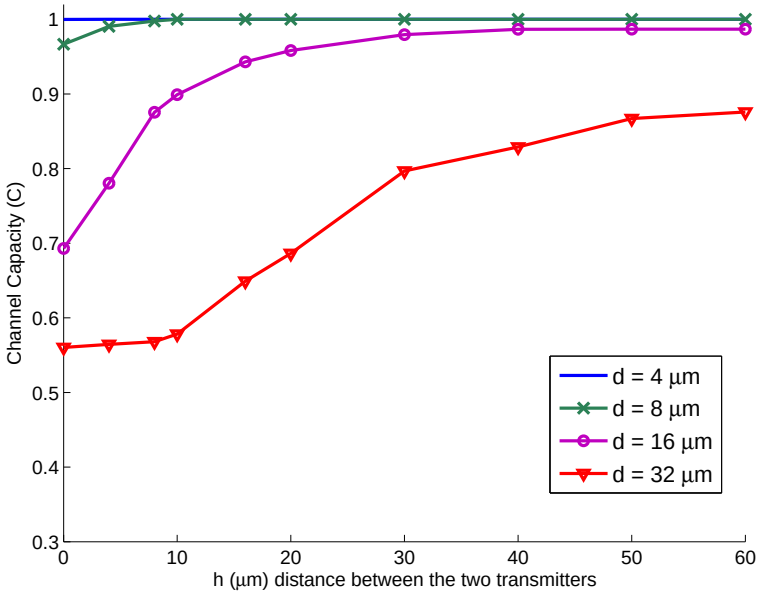

Figure 5.6. Effect of h over Channel capacity with varying d using BMoSK.

volume of the target negatively affects P_{hit}^{W}, it is compensated by the decrease in the total distance from the molecular release point and the wrong receiver. As with the previous graphics, increasing h decreases the CCI effects while increasing P_{hit}^{R}.

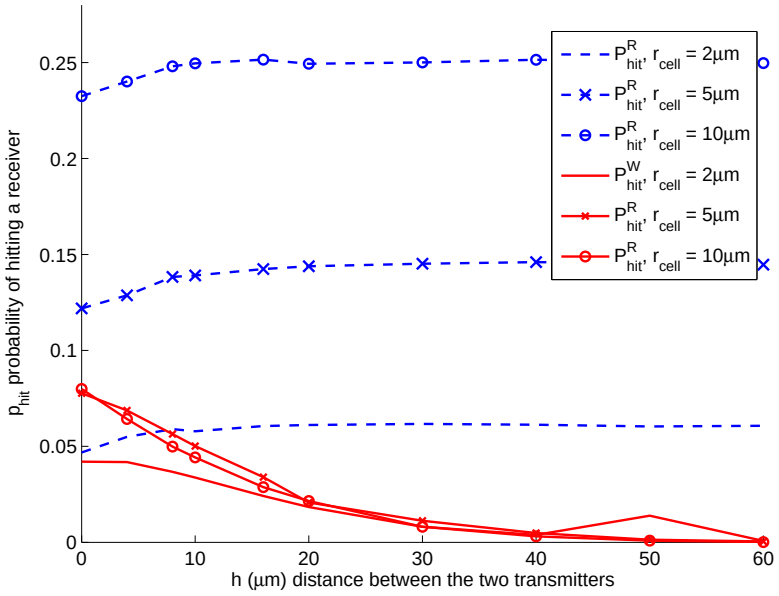

Figure 5.7. Effect of h over the hitting probabilities with varying r_{cell}.

Note that the ratio between P_{hit}^{R} and P_{hit}^{W} for $d = 32\,\mu m$ and $r = 5\,\mu m$ case in Figure 5.4 and $d = 16\,\mu m$ and $r = 2\,\mu m$ case in Figure 5.7 are very similar. Hence, there is a critical d value for a given r_{cell} after which P_{hit}^{R} and P_{hit}^{W} become very close to each other and the signal is heavily affected by the CCI due to the other transmission.

Lastly, we evaluate the effect of average power over the channel capacity for different h values with a fixed transmission range of 16 μms and r_{cell} of 5 μms. As seen in Figure 5.8, at all power levels, increasing h increases the channel capacity up to a certain value depending on the transmission range. So, the positive effect of selecting a higher h value is not affected by the average symbol power, but the average symbol power determines the upper limit for the channel capacity when h is high enough. Note that the average signal power does not change the point after which the increase in the channel capacity stops.

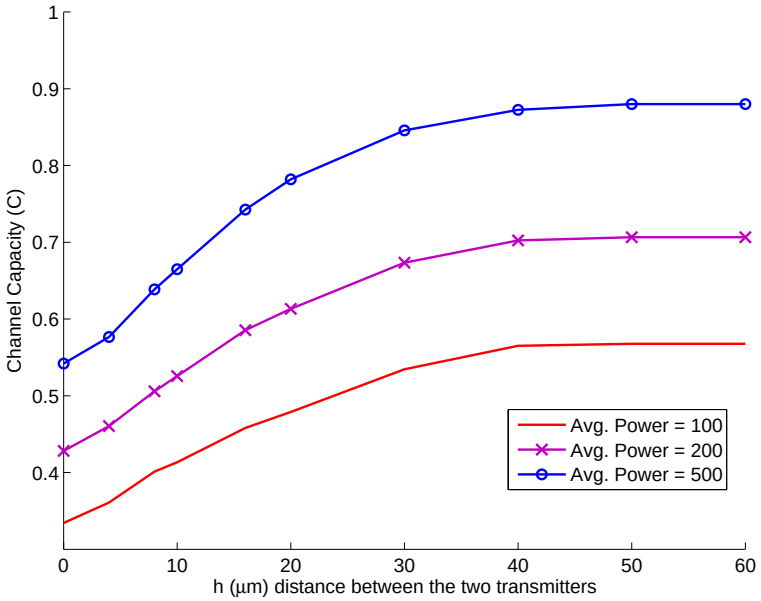

Figure 5.8. Effect of h over channel capacity with varying average symbol power.

6. ANTENNA DESIGN FOR THE CVD SYSTEM

Based on the application, the bio-nanomachines will be placed in the target environment using different placement schemes. The selection of deployment inside or outside the living organisms implies significantly different environments. Similarly, deployments inside different tissues suggest different nanonetworking topologies and transmission media capabilities. For example, a health monitoring system deployed inside the capillaries of a mammal has to take the blood flow into consideration. Thus, the range between two adjacent nanomachines can be selected larger compared to a free diffusion environment. However, in such an environment energy-wise it would be extremely ineffective to try transmitting molecules in the reverse direction to the blood flow. Thus, the transmission must follow the direction of the blood flow.

In this chapter, we consider a multi-node environment model in which bio- nanomachines are deployed close to each other (i.e., a few to tens of micrometers) to form 3D meshes of nodes. This environment can be mainly applicable to outside living organism cases since the environment is only composed of bio-nanomachines. By choosing some of the bio-nanomachines as foreign objects to the network (i.e., cells of a living organism), this topology can also reflect a deployment of bio-nanomachines inside living organism tissues. In the rest of the chapter, we use the terms bio-nanomachine and node interchangeably.

6.1. Description of the multi-node environment

In our multi-node environment model, the nodes are assumed to have a spherical size of equal radius (r_{cell}). The shortest distance between each adjacent node couple is also selected to be equal (d) for the sake of simplicity of the analysis. To attain the equidistant property while providing maximum area density, the spherical nodes should be deployed in a specific lattice. Among various lattices that conform this property, we choose the Hexagonal Close-Packed (HCP) lattice in this work (Figure 6.1). In this lattice, nodes are placed on a number of 2D planes and a given node has twelve

neighboring nodes; six in the same plane, three in one higher plane, and the last three in one lower plane. The distance between each adjacent 2D plane is equal to $\frac{2r_{cell}}{3}\sqrt{6}$.

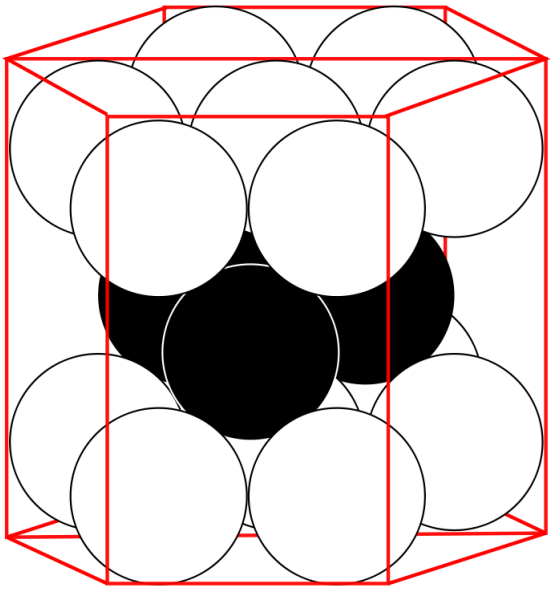

Figure 6.1. HCP lattice example, $d = 0$ (image copyright in the public domain; Courtesy of Wikipedia).

Along the boundaries of each node, there are receptors that are specific to a single type of messenger molecule. We use protein-based messenger molecules that are composed of several amino acids. Due to the chemical relationship between the messenger molecule and its receptors, nodes without the corresponding receptors cannot take in the molecule from the environment. Thus, the usage of different messenger molecules and their corresponding receptors imply an addressing structure in this communication system. The propagation dynamics are also affected from this structure since other nodes just act as an impenetrable barrier to the propagating messenger molecules. Different types of messenger molecules can be attained by changing the sequence, type, and number of amino acids of the molecule.

Receptors in the CvD systems are not passive receivers as antennas in wireless RF-based communication. The reception between the messenger molecule and its appropriate receptor is governed by specific chemical reactions. These reactions also attract stray molecules in the environment towards the receptor if the molecule is inside the affinity radius of the receptor ($r_{affinity}$). This relationship is called receptor

affinity in the biology literature [1]. Different receptor and molecule couples have different affinity capabilities and ranges. This leads to nodes having an effective radius, ($r_{effective} = r_{cell} + r_{affinity}$) in addition to their actual physical radii. Considering this phenomenon, a messenger molecule is received by its target not only if it directly hits the receiver nanomachine, but also if it enters the effective radius of the receiver. As stated above, during the communication between two nodes in multi-node environment, the remaining nodes act as obstacles. To avoid passing of molecules through these obstacles, the propagation model should be altered to reflect this limitation to the regular Brownian motion. There are several movement models in the literature that can be used for such an environment. Two of the most important movement models are Blind Ant and Myopic Ant models [47] (Figure 6.2). According to the Blind Ant model, at the end of each time step, if the new position of the molecule is illegal (i.e., inside an obstacle) the movement is rolled back. On the other hand, in the Myopic Ant model, when a molecule is close to an obstacle, its movement pattern (and therefore the normal distributions) is altered so that it cannot move to the illegal direction. In [48], Avraham *et al.* show that both models converge to the same movement pattern in the long run. We choose the Blind Ant model for our simulations since it is computationally less intense than the second model.

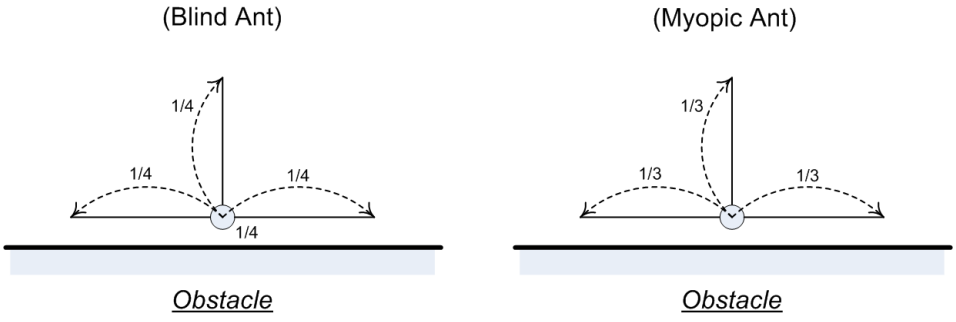

Figure 6.2. Next step probabilities in Blind and Myopic ant models in a step size 2D random walk.

6.2. Evaluation of the multi-node environment

We evaluate the performance of the CvD system in a multinode environment with nodes placed in the HCP lattice pattern as explained above. There are no boundaries in the environment. The messenger molecules are modeled after an amino acid based

molecule, the insulin hormone in the human body. The sizes of the nodes are selected based on the average size of an eukaryotic cell and the fluid in the environment is selected as water. The environment consists of three planes, and in each plane there are 49 nanomachines, distributed evenly in 7 rows and 7 columns. We use Monte Carlo simulations and evaluate the results by averaging over 10,000 trials. Other simulation parameters are given in Table 6.1. As the random number generator, we use the widely used Mersenne Twister algorithm.

Table 6.1. Simulation parameters for the multi-node environment.

Parameter	**Value**
Stokes' radius of the messenger molecule (r_s)	2.68nm
Radius of the messenger molecule (r_{mm})	2.5nm
Viscosity of the fluid (η)	0.001 $\frac{kg}{sm}$
Temperature (T)	310 K
Drag constant (b_{drag})	5.391 $10^{-11}\frac{kg}{s}$
Diffusion coefficient (D)	79.4 $\frac{\mu m^2}{s}$
Radius of the nanomachines (r_{cell})	10 μm
Simulation time	10.000 s
Plane count	3
Row/Column count	7

The results of the multi-node environment are compared to the free diffusion environment described in Chapter 2. In this free diffusion environment, the only node in the environment is the receiver and there are no obstacles that affect the propagation of the messenger molecules. In both environments, the interaction between messenger molecules (i.e., collisions, attraction, repulsion) are assumed to be negligible. As seen in Figure 6.3, the probability of hit at the receiver increases in the multi-node environment compared to the free diffusion environment. This is a direct consequence of the fact that, in the multi-node environment, the molecules released from the transmitter cannot go back through the transmitter node since it acts as an obstacle for the messenger molecules. Neighboring nodes also limit the movement of the molecules

and act as walls that compose a passage way. The sharp decrease in the hitting probabilities with the increase in d, is observed in both environments. So, even though there are obstacles that limit the movement of the molecules, communication at long distances (more than 10 μms) require the release of many molecules to be effective. Even then, the energy/bit for communication is too high for an effective transmission. Also, such a transmission generates many stray molecules in the environment, which in turn increases the noise for all nearby CvD transmissions and ISI.

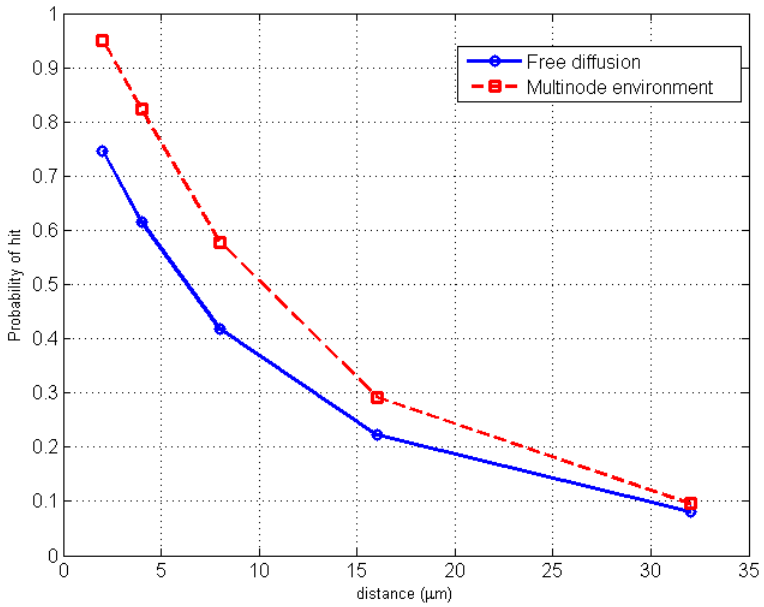

Figure 6.3. Effect of the environment on probability of hit.

In the multi-node environment, the average propagation delay of the molecules is less than that in the free diffusion environment (Figure 6.4). This decrease is also based on the obstacles in the environment since they decrease the chance that a molecule wanders around and reaches at the receiver over a long path. Also, in the multi-node environment if a molecule enters a path between several nodes, it is very unlikely that it will reach back at the receiver. Thus, avoidance of the longer paths reduces the delay.

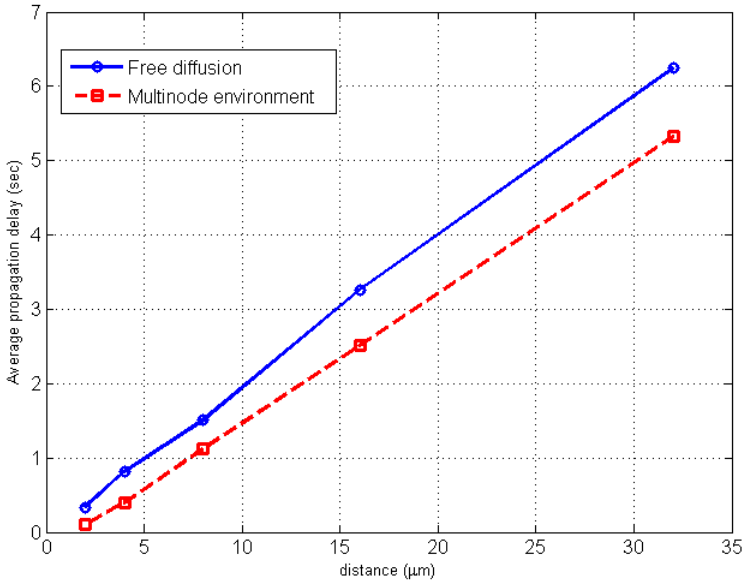

Figure 6.4. Effect of the environment on average propagation delay.

6.3. Antenna design for the CvD system

In a multi-node environment, a transmitter communicates with other nodes by using different messenger molecules that interact only with specific receptors. This can be implemented via various methods such as using proteins with different amino-acid patterns and building molecular structures in which some parts refer to the addressing information while the rest represents the data and other header information of the message.

A node can emit the messenger molecules from any part of its boundaries (i.e., release points). The selection of the release point of the messenger molecules affects the performance of the communication since it determines the distance to be traversed by the messenger molecules to reach at the receiver, especially when r_{cell} is comparable to d. As seen in the previous section, with the increase in the distance that the messenger molecules traverse, the probability of hit decreases and the average propagation delay increases. Thus, in the CvD system, in order to maximize the efficiency of the transmission, a node should select the release point which is closest to the receiver.

6.3.1. Effect of the release point

In order to show the effect of selecting different release points on the communication performance, we conduct simulations. Unlike the previous chapters, in this chapter we utilize a 2D environment instead of a 3D one due to ease of analysis regarding geometric calculations. The simulation parameters are again selected as in Table 6.1 with two different d values. The results are averaged over 30,000 trials. In addition to the previous parameters, we introduce a new parameter, α, that describes the angle between the two following lines; the line between the release point and the center of the transmitter, and the line between the centers of the transmitter and the receiver (Figure 6.5).

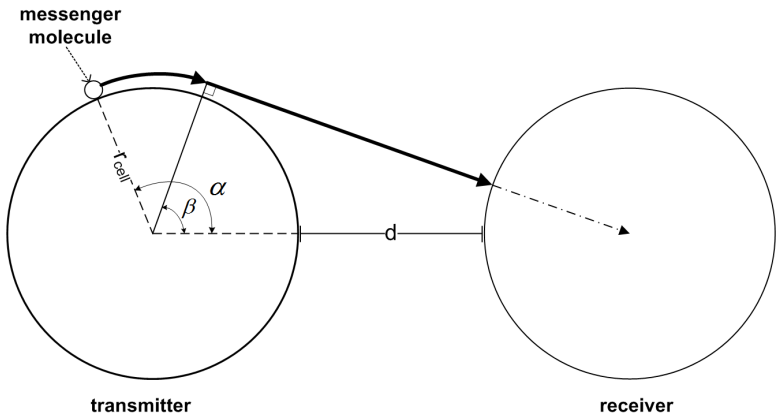

Figure 6.5. Selecting the angle between the release point and the center of the sphere.

As seen in Figure 6.6, the probability of hit sharply decreases after 30° and becomes less than 0.2 after 130°. As α increases, the shortest distance to the receiver also increases. After 90°, the molecules are forced to travel to the other side of the transmitter in order to reach the receiver, which further decreases the probability of hit values.

The average delay of the molecules is also adversely affected by the angle of the release point (Figure 6.7). If α is chosen larger than 30°, the average delay increases considerably as the angle increases.

The selection of r_{cell} also affects these two performance metrics. As r_{cell} increases,

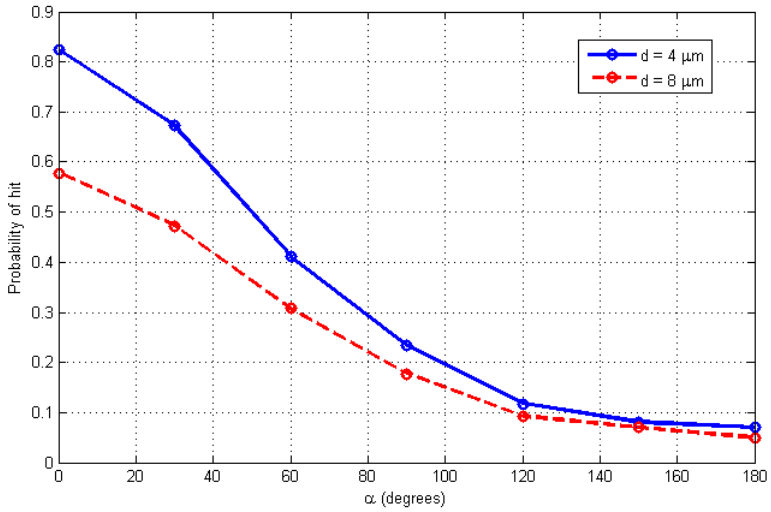

Figure 6.6. Effect of angle of the release point over probability of hit.

the performance degradation based on the selection of the release point becomes more severe since the shortest distance increases with r_{cell}. On the other hand, if the radius decreases, the effect over the performance is decreased. We select r_{cell} value as 10 μm, equal to the average size of a eukaryotic cell.

Based on these results, it is clear that selection of the appropriate release point has a significant effect over the probability of hit and the average propagation delay. Also, the stray molecules in the environment have adverse effects on other communicating pairs.

6.3.2. Benefits of a steerable antenna design in the CvD system

For a given node, the appropriate release point would be different based on the target of the transmission in question. If the node does not have any steerable antenna capability, it can employ only very simple release point selection schemes. The simplest scheme is to choose one release point for all transmissions. While this method is suitable for some of the adjacent nodes, transmission to other nodes would suffer from low hit probabilities and long average propagation delays. A more advanced scheme would be the selection of an arbitrary release point for each transmission. This scheme provides fairness among receivers to some extent, but on the average the performance of a given

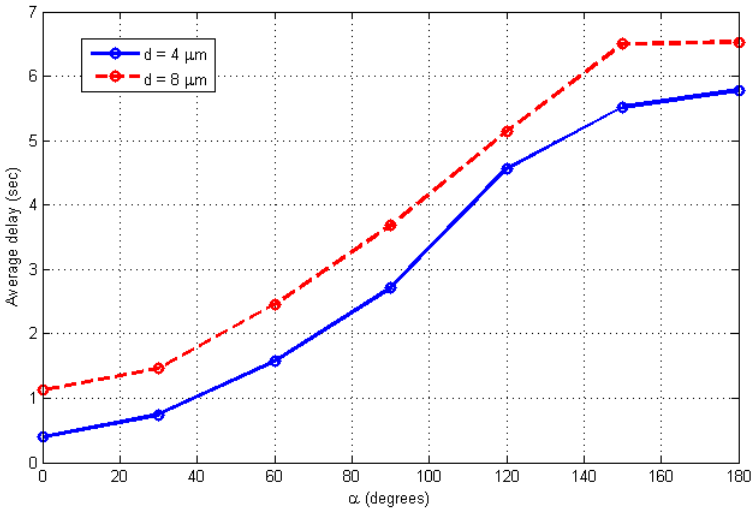

Figure 6.7. Effect of angle of the release point over average delay.

transmission would still be far from optimal.

In the arbitrary selection case, the distance a molecule has to traverse can be calculated based on the selection of the α value and denoted by $P(\alpha)$. Using trigonometric relations from Figure 6.5, this distance in a $2D$ circle can be found as

$$P(\alpha) = \begin{cases} \frac{\pi r_t(\alpha-\beta)}{180} + sin(\beta)(2r_{cell} + d) - r_t, & \alpha > \beta \\ \sqrt{f^2 + e^2} - r_t, & \alpha \leq \beta \end{cases} \tag{6.1}$$

where

$$f = sin(\alpha) \cdot r_t, \tag{6.2}$$

$$e = 2r_{cell} + d - cos(\alpha) \cdot r_t, \tag{6.3}$$

$$r_t = r_{cell} + r_{molecule}, \tag{6.4}$$

and β is the release point angle at which the straight line between the centers of the

molecule and the transmitter is perpendicular to the straight line between the centers of the molecule and the receiver (both the α and β values are in degrees). This angle is calculated as

$$\beta = arccos(\frac{r_t}{2r_{cell} + d}) \tag{6.5}$$

By integrating these paths $P(\alpha)$ over α, the average path distance can be found by using symmetry as,

$$\begin{aligned} E[P] &= \frac{1}{180} \cdot [\int_0^{\beta} (\sqrt{f^2 + e^2} - r_t) d\alpha \\ &+ \int_{\beta}^{180} (\frac{\pi r_t(\alpha - \beta)}{180} + sin(\beta)(2r_{cell} + d) - r_t) d\alpha] \end{aligned} \tag{6.6}$$

We evaluate the $E[P]$ for different d and r_{cell} values using this arbitrary scheme and compare them against the optimal distance that can be attained using a steerable antenna design. We also add another sub-optimal solution in which the steerable antenna mechanism cannot select the optimal release point but chooses points close to the optimal subject to a normal distribution (i.e., $N(0, \sigma)$ where 0° refers to the α value of the optimal release point).

Table 6.2. E[P] values (μm) using different steerable antenna schemes ($r_{cell} = 10\mu m$).

d	**Optimal**	**Sub-optimal** ($\sigma = 20$)	**Arbitrary Scheme**
$4\mu m$	4	4.925	16.287
$8\mu m$	8	8.858	19.976
$12\mu m$	12	12.812	23.840
$16\mu m$	16	16.780	27.682

As seen in Table 6.2, using the arbitrary scheme, a molecule has to traverse more than four times the d value. With the increase of d, the difference between the optimal and the arbitrary scheme results decreases since d becomes the prevalent factor in E[P]. The sub-optimal solution is used with a small σ value; therefore it gives results very close to the optimal solution. In Table 6.3, it is shown that the effect of using a steerable

antenna scheme varies based on the value of r_{cell}, as explained in Section 6.3.1. The increase in r_{cell} proportionally increases the efficiency of such an antenna mechanism. Contrarily, as r_{cell} decreases, the selection of the optimal release point turns out to be insignificant.

Table 6.3. E[P] values (μm) using different steerable antenna schemes ($d = 4\mu m$).

r_{cell}	**Optimal**	**Sub-optimal** ($\sigma = 20$)	**Arbitrary Scheme**
$1\mu m$	4	4.064	5.103
$5\mu m$	4	4.427	9.986
$10\mu m$	4	4.925	16.287
$15\mu m$	4	5.435	22.680

7. OVERVIEW OF A VARIANT MOLECULAR COMMUNICATION SYSTEM: CALCIUM SIGNALING

In Chapters 2 through 6, we have discussed several issues of the free diffusion based CvD system. As explained in Section 1.4, there are MC systems other than CvD that use a diffusion-based propagation medium. In this chapter, we give an overview of another prominent MC system called Calcium Signaling (CS). In contrast to the CvD system, the movement of the messenger molecules is not free and confined within the cell walls of the bio-nanomachines in the topology. This difference greatly affects the physical layer characteristics of the communication system and requires additional research specific for the CS system.

7.1. Intercellular Calcium Waves

As explained briefly in Section 1, The CS system is built based on the ICW phenomenon observed in a variety of biological tissues. ICW is one of the main intercellular communication systems observed among biological cells [32]. In this system, after a cell is stimulated, it generates a response to this stimulus with an increased cytosolic Ca^{2+} concentration through the usage of the secondary messenger molecule, inositol 1,4,5-triphosphate (IP_3). Then, this Ca^{2+} concentration signal is passed to the neighboring cells to form a cascading Ca^{2+} concentration wave in the vicinity of the stimulated cell. ICW is somewhat of a misnomer from a communication perspective, in the sense that what actually passes between adjacent cells is not the Ca^{2+} signal itself but the extracellular messengers (i.e., IP_3 or ATP).

7.1.1. Operational Features

The repetition of the signal among adjacent cells is achieved via two pathways: the internal pathway and the external pathway (Figure 7.1). In the former, IP_3 molecules diffuse through gap junctions, while in the latter, ATP molecules are released to the

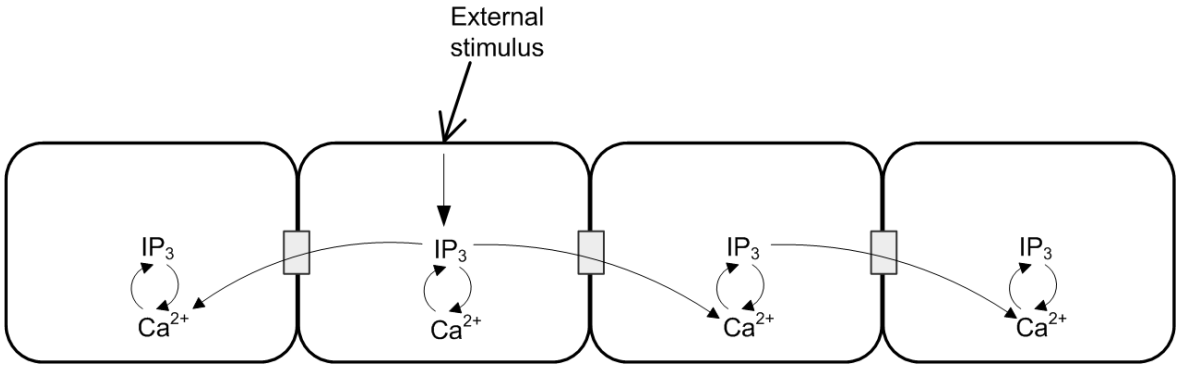

(a) *Internal pathway* mediated by IP_3 via gap junctions

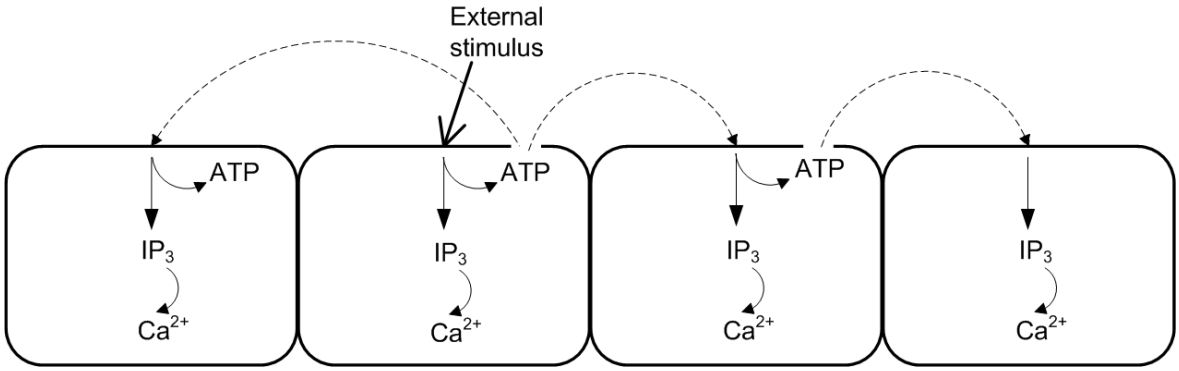

(b) *External pathway* mediated by ATP via the extracellular space

Figure 7.1. ICW pathways.

extracellular space and diffuse freely to trigger nearby cells. Gap junctions are inter-cell connections between neighboring cells located at the cell membrane. They are literally gaps that are formed out of two aligned connexon structures which connect the cytoplasm of two adjacent cells. These gap junctions allow the free diffusion of selected small molecules between these two neighboring cells. Their permeability can vary from time to time, allowing different molecules to pass between the cells. Also, they can be closed and reopened by the cell during the lifetime of a cell. According to the experimental studies, it has been shown that these pathways complement each other rather than being alternative approaches [49]. The frequency and effective range of ICW heavily depends on which pathway is used. While the internal pathway enables frequent, fast communication between nearby cells, the signal can only reach distant cells via the external pathway [49].

ICWs exist in a variety of cell tissues. While the most notable usages of ICWs are extraneuronal signal transmission by astrocytes in the central nervous system [32]

and muscle contraction by cardiac muscle tissue [50], many different cell tissues utilize ICWs as a means of intercell communication to relay different messages. Although dependent on various factors, an ICW can spread to 200-350 μm in one dimension at a speed of 15-27 μm/sec ([32, 51]) while oscillating at 10^{-3}-1 Hz range [52]. It has been shown experimentally that cells encode the information on the frequency and amplitude components of ICWs, based on the type of the cells in question [52]. The choice of calcium ions by the cells over other potential alternatives (e.g., Mg^{2+}, K^{+}, Na^{+}) is assumed to be due to the unique chemical properties of calcium that allows quick interaction with biological molecules [50, 53].

7.1.2. Mathematical Models

In the literature, many mathematical models that aim to capture the prevalent dynamics of ICWs have been proposed (e.g., [32], [51], and [54]). While some models focus on either the internal or the external pathway, others try to integrate these two pathways to form a unified model. Being a signal, it is expected that during the signal repetition, the signal should decrease in amplitude over time. However, it is observed that in some cases the signal regenerates itself while it is repeated among cells [32]. The regeneration nature of the extracellular messengers differ between models. While some models represent extracellular messengers as being regenerated at each cell along the propagation of the wave (regenerative models), others claim that these messengers are only generated at the cell in which the transmission has been started (non-regenerative models) [49]. In [52], Schuster *et al.* give a detailed survey regarding these ICW models while classifying them as deterministic or stochastic, and minimal or extended based, on the number of system parameters used in the model. According to their classification, the most important system parameters are the cytoplasmic IP_3 and Ca^{2+} concentration as well as Ca^{2+} concentration in the endoplasmic reticulum (ER), the mitochondria, and occupied calcium binding sites on the buffers in the cytosol.

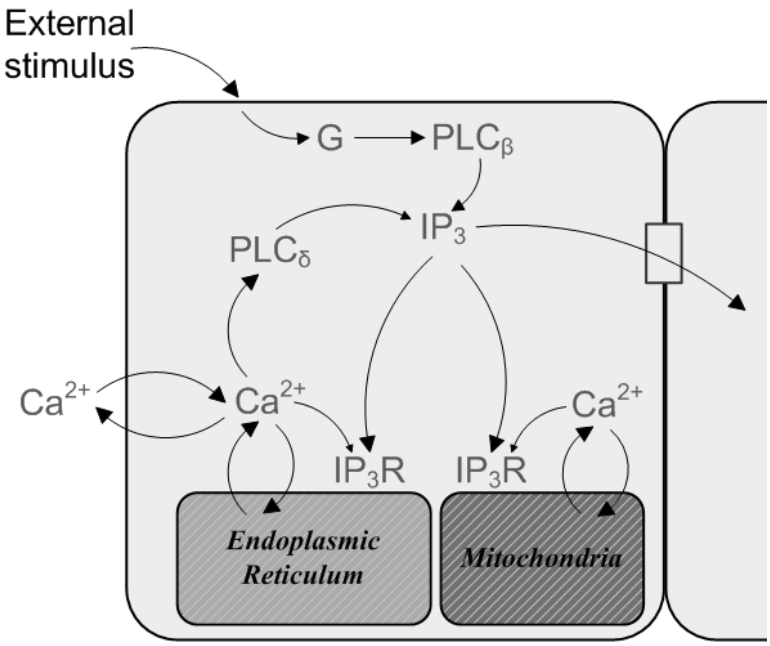

Figure 7.2. Intracellular Ca^{2+}, IP_3 dynamics.

7.1.3. Signaling Dynamics

According to these models ([32, 51, 54]), following the external stimulus, a signaling cascade occurs inside the cell that involves the organelles ER and mitochondria, which act as Ca^{2+} pools. The dynamics involved in ICW can be split into two stages: signal generation and recovery to the basal state. In the first stage, the cell generates the signal inside the cell via increasing the cytosolic Ca^{2+} concentration. After the signal is generated and forwarded to the adjacent cells, the cell returns to its original Ca^{2+} concentration level in order to prepare for a subsequent signal. The recovery stage is accomplished with mechanisms that pump the Ca^{2+} back into these pools and outside the cell.

When an external stimulus (e.g., glutamate) is received at the cell via the formation of a chemical bond between the received molecule and the receptor, the release of a G-protein is triggered (Figure 7.2). The released G-protein molecules further trigger a chemical called PLC_β, which in turn enables the release of IP_3 inside the cytosol [54]. Being highly diffusible, IP_3 molecules quickly travel inside the cell and trigger the IP_3 receptors (IP_3R) that are located on the membranes of ER and mitochondria. These

receptors open the calcium channels, and Ca^{2+} starts to diffuse into the cytosol, following the huge Ca^{2+} concentration gradient between these organelles and the cytosol (i.e., between 30-100 nM in the cytosol while 0.2-1 mM in the organelles [53]). Besides forming ICW in this first cell, the increased cytosolic Ca^{2+} concentration induces a feedback loop by enabling the release of more IP_3 molecules via triggering PLC_δ molecules [54]. This positive feedback mechanism is called Calcium Induced Calcium Release (CICR). Then, the signal propagates to adjacent cells by the passage of the IP_3 molecules through the gap junctions along the edges of the cell, and forms the internal pathway (Figure 7.1). Meanwhile, the cell releases some ATP molecules into the extracellular space, forming the external pathway. In addition to the IP_3 molecules, some Ca^{2+} molecules also pass to the neighboring cells via the gap junctions, but the rate of this transfer is extremely low [51].

After the signal is generated in the cell, the increased cytosolic Ca^{2+} concentration remains stable for a brief period of time during which the cell is irresponsive to other similar stimuli. The duration of this period varies based on the cell type in question, from several seconds to minutes ([51,54]). Then, the cell returns to its original resting (i.e., basal) cytosolic Ca^{2+} concentration level so that it can be responsive to further stimuli, and its chemical structure becomes stable again. This recovery stage is achieved via the Ca^{2+} channels and various pumps in the cell. First of all, when the cytosolic Ca^{2+} concentration passes a certain threshold, the IP_3R-gated calcium channels close down and cut off the flow of Ca^{2+} into the cytosol [49]. The excessive Ca^{2+} inside the cell is taken out of the cell via the Ca^{2+} pumps. While the majority of these excessive ions are pumped back into organelles via ER and mitochondria pumps, some are pumped out of the cell via cell membrane pumps. Meanwhile, due to a variety of reasons, the chemical bond between the receptor and the external stimulus molecule degrades and the receptor once again becomes responsive to external stimuli. Thus, the cell returns to its basal state awaiting further stimuli.

7.2. Calcium Signaling: A Molecular Communication System

Based on the ICW system, Nakano *et al.* have proposed a MC system called CS. The system is composed of two types of devices, the transmitting pair (i.e., source and destination devices) and the ICW-capable intermediary cells (Figure 7.3) [33]. Similar to other communication systems, CS is composed of three main steps: encoding, propagation, and decoding. The source device encodes the information onto an ICW wave by generating a stimulus to the closest intermediary cell in the ICW channel. Then, the calcium signal propagates through the intermediary cells via the internal and external pathways until the closest cell to the destination device is reached. Lastly, the destination device decodes the information from the last intermediary cell by sensing its cytosolic Ca^{2+} concentration and receives the message. Alternatively, the last intermediary cell may release a number of specific chemicals, which can travel the extracellular space and trigger the destination device. The information can be encoded onto either the frequency or the amplitude of the ICW signal in the channel and different bit values can be represented by sending an appropriate amount of stimulus to the first cell in the channel or by receiving such a stimulus from the last cell.

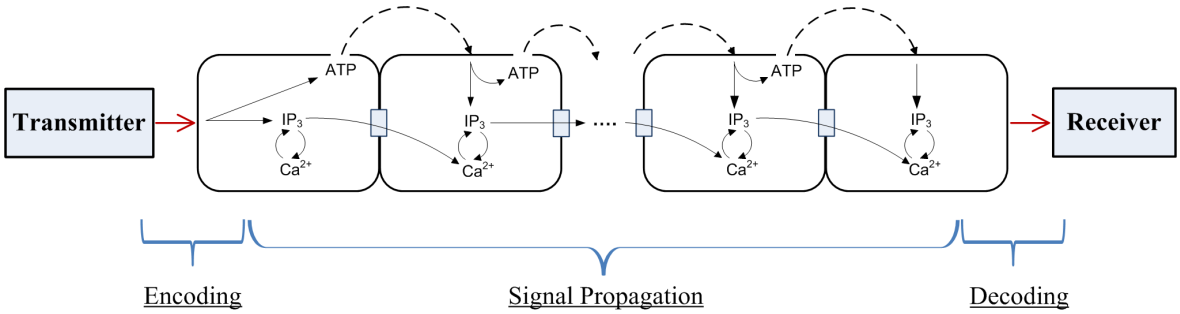

Figure 7.3. Calcium signaling.

7.2.1. Capabilities and Limitations

The main advantages of CS over other MC systems are its higher communication speed and longer operational range. As shown in previous chapters, in the CvD system as the communication distance increases, the symbol duration required to attain a high channel capacity increases exponentially.

According to Table 2.3, at 16 and 32 μm ranges, the symbol duration should be selected as 6 and 22 seconds, respectively, yielding a communication rate of 0.165 and 0.043 baud for these ranges. In the microtubular networks, molecular motors are also slow, exhibiting propagation speeds as low as 0.8 μm/s [1]. Being an intracell system, the microtubular structures are used for 10-15 μm ranges in nature. Assuming molecular motors can sustain the same propagation speed in longer ranges, it is expected to support communication rates of 0.05 and 0.025 baud for 16 and 32 μm ranges. ICWs, on the other hand, are reported to achieve higher performance, attaining speeds up to 16-27 μm/s, and ranges up to 200-350 μm [32, 51]. Therefore, a CS system is expected to give 1-1.68 and 0.5-0.84 bauds for 16 and 32 μm, respectively (without considering any interference and noise effects), surpassing both CvD and microtubule values. Besides, these values are only based on pure biological ICW capabilities. By tailoring this biological system to the required application and environment, a calcium signal might possibly exceed these values.

Another advantage of CS over CvD is the fact that, if only the internal pathway is used, the signal propagates in a protected environment. The cell membranes of the intermediary cells act as physical boundaries for the information carrying calcium ions and signal repeating secondary messenger molecules. These boundaries increase the efficiency of the diffusion by limiting the potential movement area of these molecules. Also, this dedicated channel-like structure of CS prevents the systems from any potential interference effects, such as co-channel and adjacent channel interference from other nearby CS transmissions.

On the other hand, the greatest limitation of CS is the necessity of a pre-deployed communication channel between any transmitting pair. This wire-like infrastructure requirement severely hinders any ad-hoc deployment and forces the network to be pre-configured based on the application in question. Having pre-configured infrastructure may not be crucial for an application like nanotechnology-on-a-chip in which the device is more akin to a circuit board that works outside a living organism, and the calcium channels act like the buses between the components. However, the deployment of such a pre-configured network inside a living organism may be practically difficult since the

chain of intermediary cells must be positioned across existing tissues.

Instead of a pre-configured channel, the transmitter and receiver nanomachines can be designed such that they can deploy the intermediary cells (or cell-like structures) on demand. So, before the nanomachines start communicating, they first establish a physical calcium channel by releasing some smaller cells. These cells start duplicating to reach the other device's cells. When the two cell cultures meet, the cells forming the shortest path between the devices constitute the actual communication channel. All other cells belonging to these two cultures die out using a forced programmed cell death (e.g., apoptosis). It is known that apoptosis can also be triggered via CS. Using their inherent calcium propagation capabilities these unnecessary cells can be terminated to streamline the channel.

Although ICWs are resilient against interference, they are susceptible to noise effects as observed in [52]. Thus, any CS system should take noise into account and tailor itself accordingly.

7.2.2. Research Directions

Though ICW has been studied extensively in the biology literature, there are few works that approach CS from a communication perspective. In [55], the authors use an information theoretical approach, and propose a channel capacity model for a one dimensional CS system. Although the model includes most of the prevalent Ca^{2+} dynamics in ICWs, the information relay between cells is accomplished via the ions themselves, as opposed to the usage of IP_3 molecules in biology. Therefore, the channel capacity of this model is found to be below 0.3 bits even for short transmission ranges. In [56], the authors explain a CS model designed using theoretical studies and then validate it via experiments using HeLa cell cultures. Their model includes both the Ca^{2+} and IP_3 dynamics observed in ICWs. In a more realistic experimental work, a cell wire structure between two devices has been built [57]. Similar to the previous work, programmed HeLa cell cultures have been used to form the cell wire, and the resulting structure is claimed to be stable for CS.

Table 7.1. Energy Expenditures in Calcium Signaling.

Source	**Consumed energy amount**
Stimulus triggering	1 ATP per IP_3 released
CICR (Feedback loop)	1 ATP per IP_3 released
Ca^{2+} pumps (cell membrane)	1 ATP per ion
Ca^{2+} pumps (organelle membrane)	1 ATP per ion
ATP release	Based on released ATP amount

In addition to these works, there are many issues that need to be addressed regarding CS. First of all, a complete channel capacity model should be constructed using the dynamics mentioned in the extensive ICW models in the literature. As a key component in any communication system, an energy model for CS encompassing both of the stages, signal generation and recovery to the basal state, should be developed. Following the ICW models explained above, the energy expenditures of these chemical reactions and physical channels (i.e., calcium pumps) should be calculated and a closed form solution providing the energy/bit value of the communication system should be constructed. The energy cost regarding most of the aforementioned components in Section 7.1 are known in the literature (Table 7.1). For each external stimulus molecule that triggers the release of an IP_3 molecule from the cell membrane, the cell expends one ATP molecule (roughly equal to 83 zJ) [1]. Also, in the positive feedback mechanism in the CICR, one ATP molecule is used for each IP_3 molecule released. Similarly, the pumps at both organelles' membranes and the cell's membrane spend one ATP molecule for every Ca^{2+} pumped from the cytosol [1]. In the external pathway, since ATP is used as the extracellular messenger, the cell is literally releasing energy to the extracellular environment for every ATP molecule used. Considering the high path loss rate of molecular free diffusion in the extracellular space, only a small percentage of these ATP molecules can reach the actual expected target. Thus, in order to increase the reliability of the communication channel, the device should release many ATP molecules just to mitigate this path loss rate. Apart from these straightforward expenditures, the dynamics of the feedback mechanisms (i.e., positive CICR and negative calcium channel mechanisms) should also be taken into account in order to develop a complete

energy model. There are several reaction rates in these chemical interactions that affect the propagation distance and the response time of ICWs. These reaction rates should be tuned based on the required communication range and the bit value encoded onto the current symbol. Furthermore, the number of the IP_3R gated calcium channels in the organelles and the amount of Ca^{2+} released from a single calcium channel should be evaluated based on some system parameters. Depending on the cell type, the basal cytoplasmic Ca^{2+} concentration is between 20-100 nM, and during an ICW this value rise to 400-800 nM [58]. In order to reset to its basal concentration value, the cell should spend 1 ATP molecule per Ca^{2+} for pumping purposes only. This huge energy requirement alone might push the energy budget of a CS system to very high levels. Artificially constructed cells (capable of CS) should be designed with this concern in mind, so that the overall energy budget of the communication system is kept within reasonable levels.

Another important issue is the design of the encoding and decoding parts of the system. The encoder design might follow the ICW research regarding the effects of stimulus properties (i.e., amplitude, type, frequency) over calcium signals. Thus, different types of stimulating molecules can be used with varying concentration amounts for different bit values in the symbols. For the decoder, the CvD system can be used as the last step of the whole communication. In this method, based on its cytosolic Ca^{2+} concentration, the last cell in the calcium channel converts the information into an external molecule signal, which is relayed to the receiver device. The receiver device has corresponding receptors on its cell membrane and can decode the signal into the actual information. The key issue of this signaling cascade is designing the formation of the chemical reaction chain starting from the calcium concentration to the released extracellular molecule concentration.

7.3. Deployment Scenarios

The CS system explained so far only considers a topology consisting of a pair of nanomachines. In a realistic system, there will be more than two devices in a close vicinity, and the intercommunication of these devices will require the handling of more

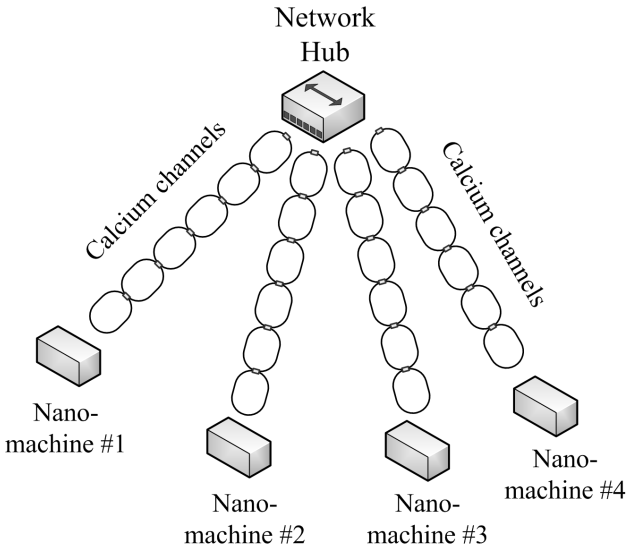

Figure 7.4. Cell Wire Star topology.

complex mechanisms (e.g., routing, medium access, scheduling). In this section, we describe three deployment schemes for CS in which there are more than two devices communicating with each other in the deployment area. In order to keep the system tractable and compatible with the core CS system, only the internal pathway of ICWs are used in the schemes explained below.

7.3.1. Cell Wire - Star Topology

This scenario extends the core CS system by allowing multiple nanomachines in the same topology and considering a star-like topology composed of user devices, intermediary cells, and a central hub-like device (Figure 7.4). In this scenario, user nanomachines are directly connected to the central hub-like device via distinct CS channels. In addition to the communication between directly connected devices, any two user devices can communicate with each other using these dedicated channels via the central device. Topology-wise, this deployment scheme is very similar to an infrastructure mode WiFi network.

Since each channel is a dedicated physical link, there cannot be any interference between any two of the channels in the topology (i.e., co-channel interference and adjacent channel interference). However, intersymbol interference can still be a problem

based on the symbol duration selection. Due to the natural calcium concentration oscillations, there can be noise in the communication channel that should be taken into account [52].

One significant issue for this kind of star-like topology is that the hub device constitutes a collision domain. One straightforward solution is to follow the well-known medium access control methods, and program the hub device to poll the user devices on a periodical basis in order to avoid any collisions. However, this will increase the average delay and energy expenditure of the network and may not be suitable for aperiodic or sporadic traffic in the user devices.

Extending the biological premise, different ions (e.g., Mg^{2+}, K^{+}, Na^{+}) can be used to enable concurrent transmissions in the topology. If the hub device can be programmed to store a received message, using different types of ions for each channel, each distinct channel can be used simultaneously in upload direction. The calcium channels are normally half-duplex channels. If the intermediary cells can be programmed to use one type of ion in the upload direction and a different type of ion in the download direction, the channel can be used in a full-duplex fashion.

Due to the multiple channel connections at the hub device, an addressing and routing mechanism is necessary in this scenario. It has been observed that ICWs originating from different cells show some minor oscillatory variations among themselves when responding to the same stimulus [49]. Using this property, instead of using different types of ions for each user device, the source address information can be encoded onto the signal itself so that the hub device can understand which nanomachine generated this signal. Also, gap junctions can alternate between open and closed states (i.e., channel gating). This channel gating can be accomplished in a few to tens of milliseconds and triggered by various methods such as voltage and chemical concentration change. Moreover, the gating of gap junctions occurs on regional basis since the voltage and chemical concentration value of every neighboring cell might be different from each other. Considering these two properties, gap junctions can be used to enforce a destination address for a signal. The hub device could be programmed to open certain

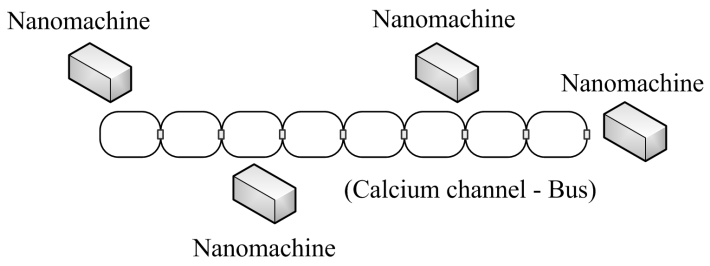

Figure 7.5. Cell Wire Bus topology.

gap junctions based on the destination address, forwarding the signal only through the calcium channel connected to the desired destination machine.

This scenario is very suitable to in vitro applications such as nanotechnology-on-a-chip in which system components require dedicated channels between themselves. The high transmission range of CS enables nanomachines that are hundreds of μms apart to communicate. They can also be used for a mediatory system between biological and man-made components (e.g., prostheses) such that both system elements are able to send/receive information using ICWs.

7.3.2. Cell Wire - Bus Topology

An alternative to the previous system could be a single bus-like cell wire to which all nanomachines in the topology are connected (Figure 7.5). In this scenario, a nanomachine that has data to transmit, triggers the cell in the channel and forms the signal representing the data. Then, the signal propagates through the whole bus structure and based on the addressing information embedded into the signal, the closest cell to the receiver decodes the information from the signal and sends it to the receiver via other MC methods (e.g. CvD).

While this scenario eliminates the need for a central device, the nanomachines require a more complex distributed medium access scheme to avoid collisions and interferences. Similar to the star topology scenario, ICW shapes can be used as a source address descriptor in this system. Kang *et al.* have observed that the shape and range of the ICWs can be tailored by altering the interaction between two key chemicals,

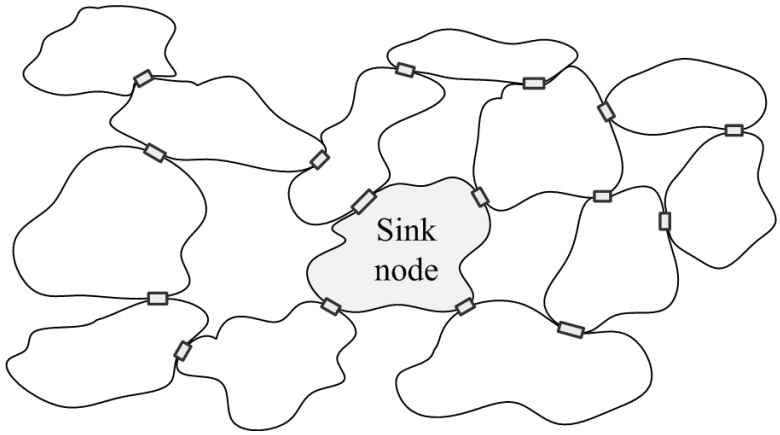

Figure 7.6. Cell Grid.

phospholipase C (PLC) and protein kinase C (PKC) [58]. This property can be used to encode the destination address to the signal itself in addition to the source address. These cell wires can be utilized as a system bus in a nanotechnology-on-a-chip design for a common information channel between several components.

7.3.3. Cell Grid

Instead of being used as intermediary cells that form the communication channel, CS-capable cells can be deployed en masse to form a grid-like structure (Figure 7.6). In this scenario, each cell acts like a nano- or micro- scale sensor that is part of a nanosensor network. Each cell is connected to other cells in the grid via gap junctions. When a sensing event occurs, the closest cells to the event generates a calcium signal that cascades through the grid and reaches the sink node in the middle which is capable of taking action accordingly. Such a deployment scenario would be suitable in vivo for detecting harmful chemicals in a noninvasive fashion. Used in vitro, such nanosensor networks can also be used for immunoassay applications to detect the existence of a certain chemical in an unknown solution or even its concentration level.

This scenario heavily exploits the broadcast nature of ICWs. However, in order to remove duplicate signals, the cells should close some of their gap junctions and use them only for reliability purposes. Thus, each node should decide which gap junctions the signal should be forwarded to. Such a path selection can be accomplished with an

adaptive technique like the Directed Diffusion method from the wireless sensor network literature. Starting from a basic flooding mechanism, using response messages in the reverse direction, the cells learn which gap junctions are more useful and reinforce them (i.e., increase the IP_3 permeability of these gap junctions) while closing others. Being a sensor network that should cover all the target environment, constructing the grid before deployment is not appropriate for such a scenario. Instead, if only the sink node is deployed, the grid can grow by cell division until its range extends to a certain distance from the sink node. Such a deployment scheme would be extremely versatile and can be designed independently from the physical topology of the target area.

Alternatively, the grid can be used for information dissemination from a central device to all connected devices for coordinating group behavior. In an application where high numbers of a certain chemical need to be released into the environment, a single device might only be capable of releasing a small number of molecules and many cells must act in unison to attain the desired molecular concentration. By synchronizing their secretion processes via CS from a central entity, the grid can act as a group and the required amount of chemical can be attained via cooperation among the cells in the grid. Such a grid can be used in synthetic tissue engineering as a possible solution for patients with partial or complete pancreas failures. Based on this scenario, artificial pancreas tissues can be engineered to act as one entity while remaining bio-compatible. Again, the broadcast nature of CS is very suitable for such an application.

8. CONCLUSION AND FUTURE DIRECTIONS

Communication via Diffusion is a new system that is still at its infancy. Currently, there are many issues that has to be addressed in order to flesh it out as a complete communication solution. While some of these issues deal with basic signaling (e.g., modulation, coding, transmitter and receiver design) others are higher layer mechanisms (e.g., multiple access, addressing, routing). In this thesis, among these issues we focused on mostly physical layer issues which will establish the basic signaling level of this system.

Main contributions of this thesis can be outlined as below

(i) *Joint energy and channel model*: Unlike most of the traditional communication systems, the communication medium of the CvD system is probabilistic. This property alone requires revisiting of the whole channel modeling and capacity analysis for this system. While there are some channel models proposed in the literature, all of them lack critical system constraints such as energy requirement and use system parameters that are unsuitable for in vivo environments. In this thesis, we have developed the first joint energy and channel model for the CvD system and calculate a rough estimate of the energy cost of data transmission using this system. In our model, we use the energy consumption experienced by the pancreatic $\beta - cells$ as a starting point in order to make the analysis as realistic as possible to in vivo environments. We also show that, with the current free diffusion medium the performance of the CvD system is limited to short-to-medium ranges up to 10 μms.

(ii) *Modulation techniques*: In the initial proposal of the CvD system, the information is encoded upon the concentration level of the messenger molecules released to the environment. We generalized this modulation technique, as we call it the Concentration Shift Keying - CSK, by using different number of threshold values for carrying more than a single bit per symbol. As an alternative, we proposed the Molecular Shift Keying - MoSK, a modulation technique unique to this

specific medium that encodes the information upon the type of the messenger molecule released to the environment. We compared these two techniques and show that MoSK is more resilient to noise and low power per symbol than the CSK technique.

(iii) *Interference analysis*: As any communication system, the CvD is also expected to experience some interference both from nearby other transmissions and the multi-path components of the signal itself. We show the effects of both ISI and CCI over the performance of the CvD system and propose solutions to reduce the destructive effects of these interferences by tailoring the symbol duration and minimum distance between nearby bio-nanomachine pairs values according to the distance and power of the transmission in question.

(iv) *Antenna design and release point selection*: Lastly, we show the effects of selecting the release point of the messenger molecules over the performance of the system. Since the performance of the system is greatly hindered by the distance between the communicating pair, it is shown that unlike the electromagnetic communication systems, usage of a steerable antenna and choosing the closest molecular release point to the receiver is of paramount importance to the average delay and reliability of the communication system.

As the continuation of this work in the future, we plan to work on other diffusion based systems, such as the Calcium Signaling in which the propagation environment is constrained by the cells themselves. Such constrained environments are known to extend the range of the communication greatly while requiring more complex signalization mechanisms. We also plan to work on a channel based CvD systems in which, the propagation of the messenger molecules is again constrained (and therefore passively guided) based on the neuromuscular junction between the nerve and muscle cells. While this channel based CvD variant is expected to consume much more energy than the regular CvD system, based on our initial findings, the propagation delays are expected to be one third of one fourth of the delay experienced in the regular CvD system.

REFERENCES

1. Alberts, B., A. Johnson, J. Lewis, M. Raff, K. Roberts and P. Walter, *Molecular Biology of the Cell*, Garland Science, New York, NY, USA, 5th edn., 2007.

2. Baluska, F., D. Volkmann and P. W. Barlow, *Cell-Cell Channels*, Landes Bioscience, Georgetown, TX, USA, 2006.

3. Feynman, R., "There's Plenty of Room at the Bottom", *Caltech Engineering and Science*, Vol. 23, 1960.

4. Moore, G. E., "Cramming More Components onto Integrated Circuits", *Electronics*, Vol. 38, No. 8, pp. 114–117, 1965.

5. Taniguchi, N., "On the Basic Concept of 'Nano-Technology'", *Bulletin of the Japan Society of Precision Engineering*, pp. 18–23, 1974.

6. Drexler, E., *Engines of Creation: The Coming Era of Nanotechnology*, Anchor, USA, 1987.

7. Akyildiz, I. F., F. Brunetti and C. Blazquez, "Nanonetworks: A new communication paradigm", *Elsevier Computer Networks*, Vol. 52, No. 12, pp. 2260–2279, 2008.

8. Freitas, R. A., *Nanomedicine, Vol. I: Basic Capabilities*, Landes Bioscience, 1st edn., 1999.

9. Nakano, T., M. J. Moore, F. Wei, A. V. Vasilakos and J. Shuai, "Molecular Communication and Networking: Opportunities and Challenges", *NanoBioscience, IEEE Transactions on*, Vol. 11, No. 2, pp. 135–148, 2012.

10. Benenson, Y. and E. Shapiro, *Molecular Computing Machines*, pp. 2043–2055,

Taylor & Francis, 2004.

11. Jornet, J. M. and I. F. Akyildiz, "Channel Capacity of Electromagnetic Nanonetworks in the Terahertz Band", *Communications (ICC), 2010 IEEE International Conference on*, pp. 1–6, IEEE, 2010.

12. Akyildiz, I. F. and J. M. Jornet, "Electromagnetic Wireless Nanosensor Networks", *Nano Communication Networks*, Vol. 1, No. 1, pp. 3–19, 2010.

13. Jornet, J. M. and I. F. Akyildiz, "Channel Modeling and Capacity Analysis for Electromagnetic Wireless Nanonetworks in the Terahertz Band", *Wireless Communications, IEEE Transactions on*, Vol. 10, No. 10, pp. 3211–3221, 2011.

14. Jornet, J. M. and I. F. Akyildiz, "Joint Energy Harvesting and Communication Analysis for Perpetual Wireless Nanosensor Networks in the Terahertz Band", *Nanotechnology, IEEE Transactions on*, Vol. 11, No. 3, pp. 570–580, 2012.

15. Jornet, J. M., J. Capdevila Pujol and J. Solé Pareta, "PHLAME: A Physical Layer Aware MAC protocol for Electromagnetic nanonetworks in the Terahertz Band", *Nano Communication Networks*, Vol. 3, No. 1, pp. 74–81, 2012.

16. Cid-Fuentes, R. G., J. M. Jornet, I. F. Akyildiz and E. Alarcon, "A Receiver Architecture for Plulse-based Electromagnetic Nanonetworks in the Terahertz Band", *Communications (ICC), 2012 IEEE International Conference on*, pp. 1–6, IEEE, May 2012.

17. Suda, T., M. J. Moore, T. Nakano, R. Egashira and A. Enomoto, "Exploratory Research on Molecular Communication between Nanomachines", *Genetic and Evolutionary Computaion Conference, (GECCO '05)*, ACM, 2005.

18. Atakan, B. and O. Akan, "On Channel Capacity and Error Compensation in Molecular Communication", *Springer Transaction on Computational System Biology*, Vol. 10, pp. 59–80, 2008.

19. Atakan, B. and O. B. Akan, "Deterministic capacity of information flow in molecular nanonetworks", *Nano Communication Networks*, Vol. 1, No. 1, pp. 31–42, 2010.

20. Mahfuz, M. U., D. Makrakis and H. T. Mouftah, "On the characterization of binary concentration-encoded molecular communication in nanonetworks", *Nano Communication Networks*, Vol. 1, No. 4, pp. 289–300, 2010.

21. Moore, M. J., T. Suda and K. Oiwa, "Molecular Communication: Modeling Noise Effects on Information Rate", *IEEE Transactions on NanoBioscience*, Vol. 8, No. 2, pp. 169–180, 2009.

22. Pierobon, M. and I. F. Akyildiz, "A physical end-to-end model for molecular communication in nanonetworks", *IEEE Journal on Selected Areas in Communications*, Vol. 28, No. 4, pp. 602–611, 2010.

23. Llatser, I., E. Alarcon and M. Pierobon, "Diffusion-based channel characterization in molecular nanonetworks", *Computer Communications Workshops (INFOCOM WKSHPS), 2011 IEEE Conference on*, pp. 467–472, IEEE, 2011.

24. Chou, C. T., "Molecular circuits for decoding frequency coded signals in nanocommunication networks", *Nano Communication Networks*, Vol. 3, No. 1, pp. 46–56, 2012.

25. Kuran, M. S., H. B. Yilmaz, T. Tugcu and I. F. Akyildiz, "Modulation Techniques for Communication via Diffusion in Nanonetworks", *2011 IEEE International Conference on Communications (ICC)*, pp. 1–5, IEEE, 2011.

26. Pierobon, M. and I. F. Akyildiz, "Noise Analysis in Ligand-Binding Reception for Molecular Communication in Nanonetworks", *Signal Processing, IEEE Transactions on*, Vol. 59, No. 9, pp. 4168–4182, 2011.

27. Pierobon, M. and I. F. Akyildiz, "Diffusion-Based Noise Analysis for Molecu-

lar Communication in Nanonetworks", *Signal Processing, IEEE Transactions on*, Vol. 59, No. 6, pp. 2532–2547, 2011.

28. Kuran, M. S., H. B. Yilmaz and T. Tugcu, "Effects of routing for communication via diffusion system in the multi-node environment", *Computer Communications Workshops (INFOCOM WKSHPS), 2011 IEEE Conference on*, pp. 461–466, IEEE, 2011.

29. Moore, M. J. and T. Nakano, "Synchronization of Inhibitory Molecular Spike Oscillators", *Bio-Inspired Models of Network, Information and Computing Systems, (BIONETICS '11). 6th International Conference on*, pp. 183–195, 2011.

30. Moore, M. J. and T. Nakano, "Addressing by beacon distances using molecular communication", *Nano Communication Networks*, Vol. 2, No. 2-3, pp. 161–173, 2011.

31. Enomoto, A., M. J. Moore, T. Nakano, R. Egashira and T. Suda, "A Molecular Communication System Using a Network of Cytoskeletal Filaments", *Nanotechnology Conference and Trade Show, (NANOTECH '06), 9th*, pp. 725–728, 2006.

32. Scemes, E. and C. Giaume, "Astrocyte Calcium Waves: What They are and What They Do.", *Glia*, Vol. 54, No. 7, pp. 716–725, 2006.

33. Nakano, T., T. Suda, M. J. Moore, R. Egashira, A. Enomoto and K. Arima, "Molecular Communication for Nanomachines Using Intercellular Calcium Signaling", *5th IEEE Conference on Nanotechnology, 2005. (IEEE-NANO '05)*, Vol. 2, pp. 478–481, 2005.

34. Giné, L. P. and I. F. Akyildiz, "Molecular Communication Options for Long Range Nanonetworks", *Elsevier Computer Networks*, Vol. 53, No. 16, pp. 2753–2766, Aug. 2009.

35. Garralda, N., I. Llatser, A. Cabellos-Aparicio and M. Pierobon, "Simulation-based

evaluation of the diffusion-based physical channel in molecular nanonetworks", *Computer Communications Workshops (INFOCOM WKSHPS), 2011 IEEE Conference on*, pp. 443–448, IEEE, 2011.

36. Saxton, M. J., "Modeling 2D and 3D diffusion.", *Methods in molecular biology (Clifton, N.J.)*, Vol. 400, pp. 295–321, 2007.

37. Tyrrell, H. J. V., *Diffusion in Liquids: A Theoretical and Experimental Study (Monographs in Chemistry)*, Butterworth-Heinemann, 1984.

38. Cover, T. M. and J. A. Thomas, *Elements of Information Theory*, Wiley-Interscience, 2nd edn., 1991.

39. Alfano, G. and D. Miorandi, "On Information Transmission Among Nanomachines", *ICST/ACM 1st International Conference on Nano-Networks, (Nano-Net '06)*, 2006.

40. Seki, T., H. Kanbayashi, S. Chono, Y. Tabata and K. Morimoto, "Effects of a Sperminated Gelatin on the Nasal Absorption of Insulin", *International Journal of Pharmaceutics*, Vol. 338, No. 1-2, pp. 213–218, 2007.

41. Kuran, M. S., H. B. Yilmaz, T. Tugcu and B. Özerman, "Energy model for communication via diffusion in nanonetworks", *Elsevier Nano Communication Networks*, Vol. 1, No. 2, pp. 86–95, 2010.

42. Bermek, E., R. Nurten, D. Tiryaki and S. Gökçe, *Biophysics Lecture Notes (in Turkish)*, Vol. 4097, İstanbul University Press, 2nd edn., 1997.

43. Lehninger, A. L., D. L. Nelson and M. M. Cox, *Principles of Biochemistry*, W.H. Freeman & Company, 3rd edn., 2000.

44. Eliasson, L., F. Abdulkader, M. Braun, J. Galvanovskis, M. B. Hoppa and P. Rorsman, "Novel Aspects of the Molecular Mechanisms Controlling Insulin Secretion",

The Journal of physiology, Vol. 586, No. 14, pp. 3313–3324, 2008.

45. Sasaki, Y., M. Hashizume, K. Maruo, N. Yamasaki, J. Kikuchi, Y. Moritani, S. Hiyama and T. Suda, "Controlled Propagation in Molecular Communication Using Tagged Liposome Containers", *ACM 1st International Conference on Bio-inspired Models of Network, Information and Computing Systems, (BIONETICS '06)*, p. 20, ACM, New York, NY, USA, 2006.

46. Kuran, M. S., H. B. Yilmaz and T. Tugcu, "Co-channel Interference for Communication via Diffusion System in Molecular Communication", *ICST 6th International Conference on Bio-inspired Models of Network, Information and Computing Systems, (BIONETICS '11)*, pp. 199–212, 2011.

47. Havlin, S. and D. Ben-Avraham, "Diffusion in disordered media", *Advances in Physics*, Vol. 36, No. 6, pp. 695–798, 1987.

48. ben Avraham, D. and S. Havlin, *Diffusion and Reactions in Fractals and Disordered Systems (Cambridge Nonlinear Science Series)*, Cambridge University Press, 1st edn., 2000.

49. Kang, M. and H. G. Othmer, "Spatiotemporal characteristics of calcium dynamics in astrocytes", *Chaos: An Interdisciplinary Journal of Nonlinear Science*, Vol. 19, No. 3, pp. 037116+, 2009.

50. Carafoli, E., L. Santella, D. Branca and M. Brini, "Generation, control, and processing of cellular calcium signals.", *Critical reviews in biochemistry and molecular biology*, Vol. 36, No. 2, pp. 107–260, 2001.

51. Iacobas, D. A., S. O. Suadicani, D. C. Spray and E. Scemes, "A Stochastic Two-Dimensional Model of Intercellular Ca2+ Wave Spread in Glia", *Biophysical Journal*, Vol. 90, No. 1, pp. 24–41, 2006.

52. Schuster, S., M. Marhl and T. Höfer, "Modelling of simple and complex calcium os-

cillations. From single-cell responses to intercellular signalling.", *European journal of biochemistry / FEBS*, Vol. 269, No. 5, pp. 1333–1355, 2002.

53. Verkhratsky, A., J. J. Rodríguez and V. Parpura, "Calcium signalling in astroglia", *Molecular and Cellular Endocrinology*, 2011.

54. Höfer, T., L. Venance and C. Giaume, "Control and Plasticity of Intercellular Calcium Waves in Astrocytes: A Modeling Approach", *The Journal of Neuroscience*, Vol. 22, No. 12, pp. 4850–4859, 2002.

55. Nakano, T. and J.-Q. Liu, "Design and Analysis of Molecular Relay Channels: An Information Theoretic Approach", *IEEE Transactions on NanoBioscience*, Vol. 9, No. 3, pp. 213–221, 2010.

56. Nakano, T., J. Shuai, T. Koujin, T. Suda, Y. Hiraoka and T. Haraguchi, "Biological excitable media based on non-excitable cells and calcium signaling", *Nano Communication Networks*, Vol. 1, No. 1, pp. 43–49, 2010.

57. Nakano, T., Y.-H. Hsu, W. C. Tang, T. Suda, D. Lin, T. Koujin, T. Haraguchi and Y. Hiraoka, "Microplatform for intercellular communication", *Nano/Micro Engineered and Molecular Systems, 2008. NEMS 2008. 3rd IEEE International Conference on*, pp. 476–479, IEEE, 2008.

58. Kang, M. and H. G. Othmer, "The variety of cytosolic calcium responses and possible roles of PLC and PKC.", *Physical biology*, Vol. 4, No. 4, pp. 325–343, 2007.